CHAPTER IV

RESULTS AND DISCUSSIONS

4.1 Mixer test

The torque required for mixing molten parent polymers, i.e. PA6 and HiPS, is measured by using an internal mixer. Relative melt viscosity were calculated as shown in Table 4.1.

Table 4.1: Torque and relative melt viscosity of PA6 and HiPS at each mixing condition.

Condition		Torque at 10 min. (Nm)		Relative melt viscosity	
Temp.(°C)	Speed (rpm)	PA6	HiPS	PA6	HiPS
225	30	1.9	5.3	1	2.79
235	50	2.0	5.2	1	2.60
255	50	1.7	4.4	1	2.40

The distribution and the degree of dispersion of molten polymer blend is believed to depend on two dimensionless parameters, i.e. the Weber number (We) and the viscosity ratio (P).

By assuming Newtonian system with dispersed droplet deformed in a simple shear flow, the behaviour of the droplets was reported by G. Serpe, J. Jarrin and F. Dawans [15] to be mainly governed by the Weber number (We) and the viscosity ratio (P). Weber number is

defined as the actual ratio of the disruptive shearing force ($\eta_m\gamma$) and the cohesive interfacial forces (σ/R) as shown in Equation 4.1.

$$We = \eta_m R\gamma/\sigma \qquad (4.1)$$

where η_d viscosity of the matrix

η_m viscosity of the droplet

γ shear rate

σ interfacial tension

R radius of the droplet

1

2

3

4, R.-T. P. p27

5

6

7

8

9

(A) (B)

Figure 4.1: The sequence of the breakup of droplets in a simple shear field.

Figure 4.1 shows the sequence of the breakup of droplets in a simple shear field. The deformation D of a droplet is given by the ratio (L-B)/ (L+B), where L is the major axis and B is the minor axis of the ellipsoidal deformed droplet in the shear field.

The viscosity ratio, can be estimated as shown in Equation 4.2

$$P = \eta_d/\eta_m \qquad (4.2)$$

where P viscosity ratio

The influence of the viscosity ratio with respect to the droplet breakup in a system of two immiscible fluids is shown in Figure 4.1. Figure 4.1(A) shows the mechanism of droplet breakup at different levels of the viscosity ratio and Figure 4.1(B) shows the critical deformation (D) required for a drop to disperse at a minimum D when the viscosity ratio approaches unity.

The results obtained in Table 4.1 show that the relative viscosity of each polymer does not change significantly at each condition. The condition that gives a high viscosity and torque shear will be chosen. However, there is more possibility that the high temperature polymer will degrade if it is mixed at very high temperature. So a compromise condition of 235°C for mixing temperature and a mixing speed of 50 rpm is chosen to operate in melt blend on twin screw extruder.

In studying PVC by using the internal mixer, the homogeneous molten polymer time is approximated from the rise of the torque that comes from crosslinking of PVC [16]. However, neither the PA6 nor the HiPS reacts or forms crosslinks. So a constant torque is assumed to relate to homogeneity and the time taken for the constant torque to be

attained is believed to be the appropriate molten mixing time. Figure 4.2 shows the torque diagram obtained from the mixer. The appropriate homogeneous molten mixing time was determined to be about 4 min.

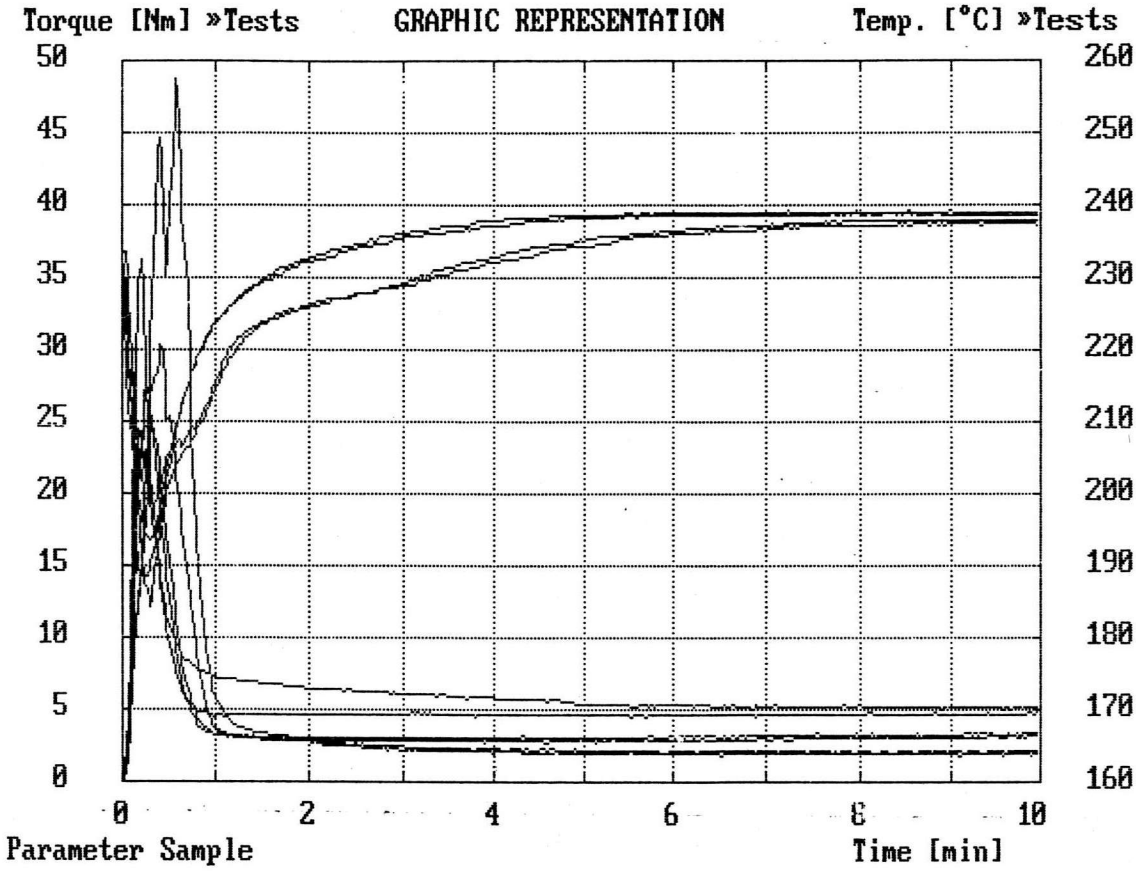

Figure 4.2: The torque-time diagram of melt mixing of uncompatibilized PA6/HiPS blends.

The resident time in the twin-screw extruder is calculated from Equation 4.3.

$$T = 3/2 * t_{homogeneous} \qquad (4.3)$$

where T resident time in twin-screw extruder

$t_{homogeneous}$ homogeneous molten mixing time

In twin screw extruder, carbon black was used as a tracer to measure the resident time of molten mixture therein. A feed of dry blend at a rate of about 20 g/min was used. The mix temperature was 235 °C and the screw speed was 50 rpm. The resident time was found to be 5 to 7 min.

4.2 Mechanical Properties

4.2.1 Effect of compatibilizer content on parent polymer

The compatibilizer used in this study is maleated styrene-ethylene/butylene-styrene block copolymer(SEBS-g-MA).

In this section, a study is conducted on the effect of the compatibilizer content on parent polymer. Various amount of SEBS-g-MA were added to HiPS and PA6. The results are presented and discussed in the following section.

4.2.1.1 Tensile properties

Figure 4.3 shows the different tensile test diagrams for PA6 and HiPS with and without the compatibilizer.

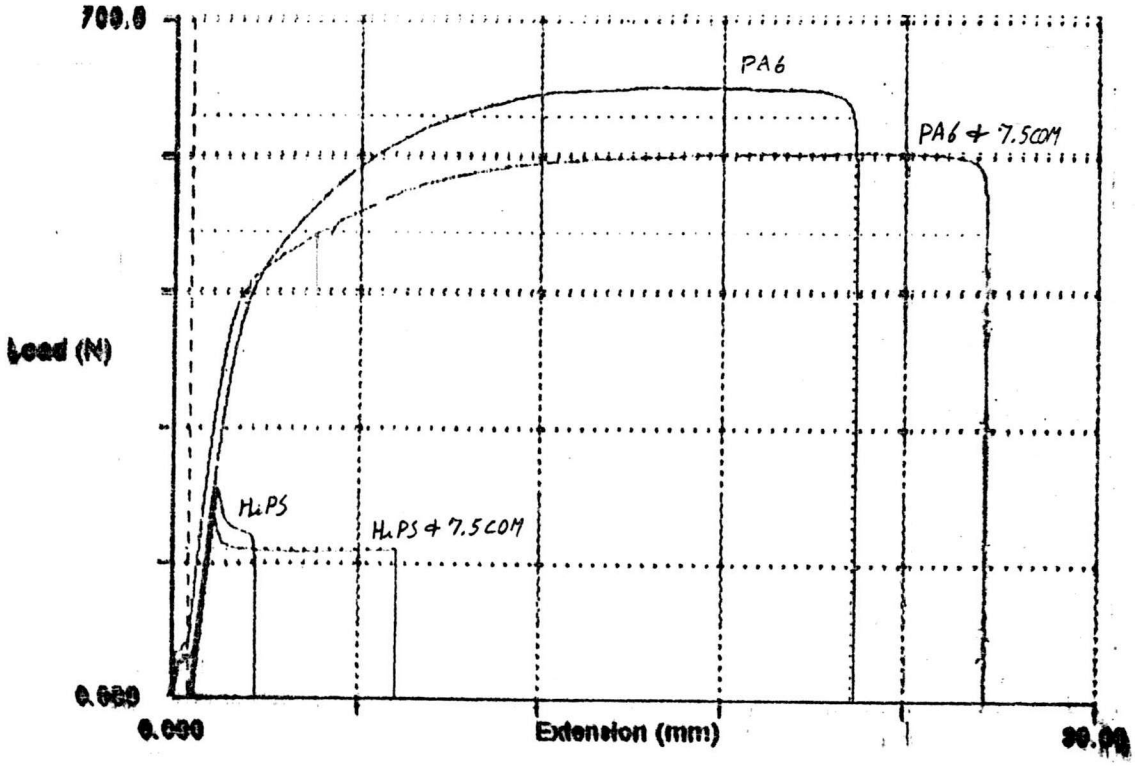

Figure 4.3: The load-deformation diagram from tensile test of PA6 and HiPS with and without the compatibilizer.

The effect of the compatibilizer content on the tensile elastic modulus, 0.2% offset yield tensile stress, 0.2% offset yield tensile strain, tensile stress at break, tensile strain at break and the tensile work done of PA6 and HiPS are shown in Figures 4.4 to 4.9 respectively.

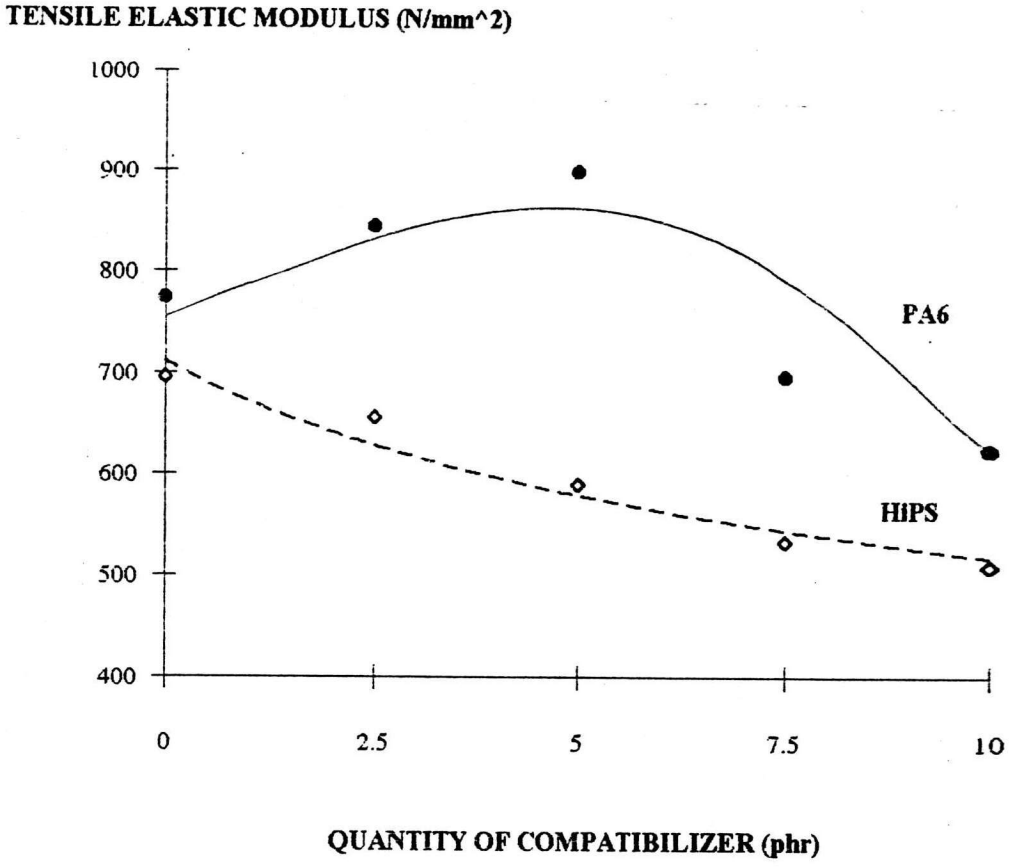

Figure 4.4: The tensile elastic modulus of compatibilized PA6 and HiPS plotted against the compatibilizer (SEBS-g-MA) concentration.

As shown in Figure 4.4, the tensile elastic modulus of HiPS decreases gently when the quantity of the compatibilizer increases while the tensile elastic modulus of PA6 increases gradully over the applied range from 0 to 5 phr of SEBS-g-MA. But beyond 5 phr, the modulus decreases abruptly.

For HiPS, when 2.5-10 phr of SEBS-g-MA was added, the tensile elastic modulus drops. At 2.5, 5, 7.5 and 10 phr of SEBS-g-MA the tensile elastic modulus decreases by 5.6, 15.2, 23.3 and 26.8%. For

PA6, when 2.5-10 phr of SEBS-g-MA was added, the tensile elastic modulus is elevated. At 2.5 and 5 phr of SEBS-g-MA, the tensile elastic modulus increases by 9.1 and 16.2%. For the range studied, when the amount of SEBS-g-MA is increased up to 7.5 and 10 phr, the modulus is found to lower. At 7.5 and 10 phr of SEBS-g-MA, the tensile elastic modulus decreases by 10.1% and 19.5%.

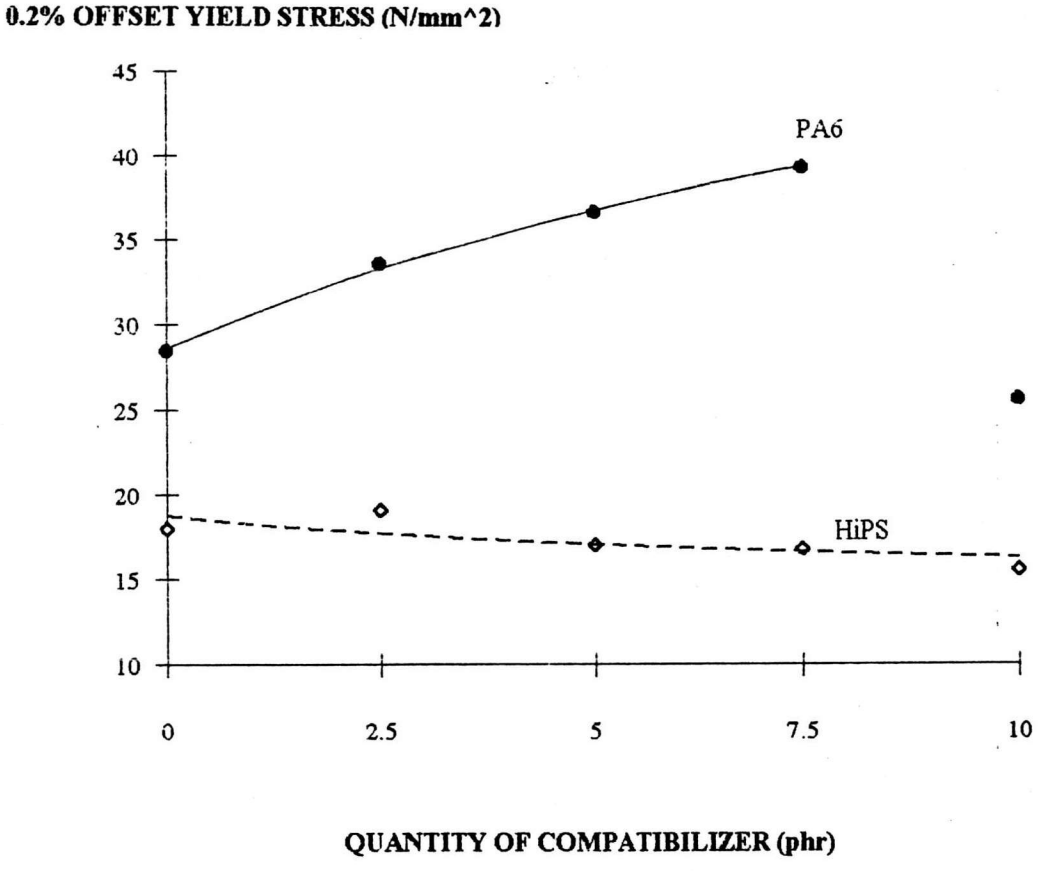

Figure 4.5: The 0.2% offset yield tensile stress of compatibilized PA6 and HiPS plotted against the SEBS-g-MA concentrations.

The 0.2% offset tensile yield stress of HiPS and PA6 is plotted against the amount of SEBS-g-MA in Figure 4.5. The 0.2% offset tensile yield stress of HiPS decreases gently when the quantity of the compatibilizer increases while the 0.2% offset tensile yield stress of PA6 increases gradually over the applied range from 0 to 7.5 phr of SEBS-g-MA. But beyond 7.5 phr, it decrease abruptly.

For HiPS, with 5, 7.5 and 10 phr of SEBS-g-MA, the 0.2% offset tensile yield stress decreases by 5.2, 6.6 and 13.5%. For PA6, with 2.5, 5 and 7.5 phr of SEBS-g-MA, the 0.2% offset tensile yield stress increases by 17.9, 28.2 and 37.7%. When the amount of SEBS-g-MA is increased up to 10 phr, the 0.2% offset tensile yield stress is found to be lower. At 10 phr of SEBS-g-MA, the 0.2% offset tensile yield stress decreases by 10.3%.

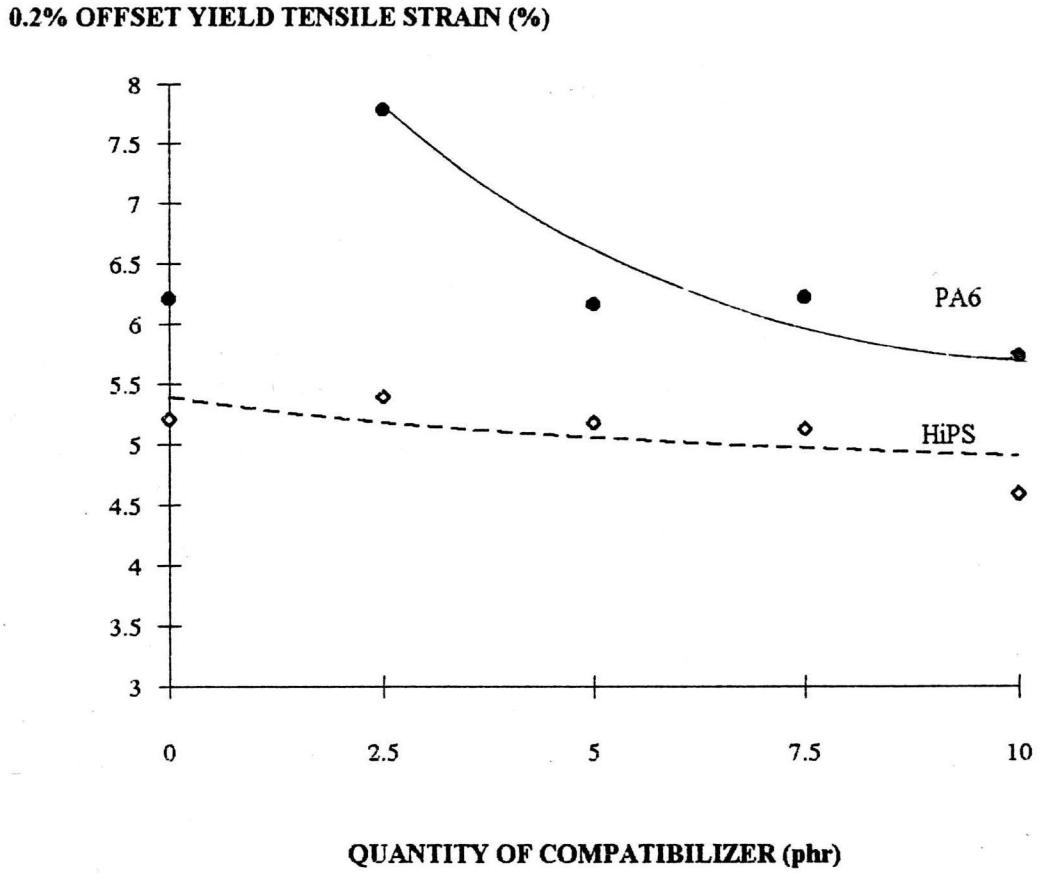

Figure 4.6: The 0.2% offset tensile yield strain of compatibilized PA6 and HiPS plotted against the SEBS-g-MA concentrations.

As shown in Figure 4.6, the 0.2% offset tensile yield strain of HiPS and PA6 have a similar trend, i.e. the 0.2% offset tensile yield strain decreases when the concentration of SEBS-g-MA increases.

For both the HiPS and the PA6, with 2.5 phr of SEBS-g-MA, the 0.2% offset tensile yield strain increases by 3.6% for HiPS and 25.5% for PA6. There is less than 2% change when 5 and 7.5 phr of SEBS-g-MA was used. For both the HiPS and the PA6, with 10 phr of

SEBS-g-MA, the 0.2% offset tensile yield strain decreases by 11.9% for HiPS and 7.7% for PA6.

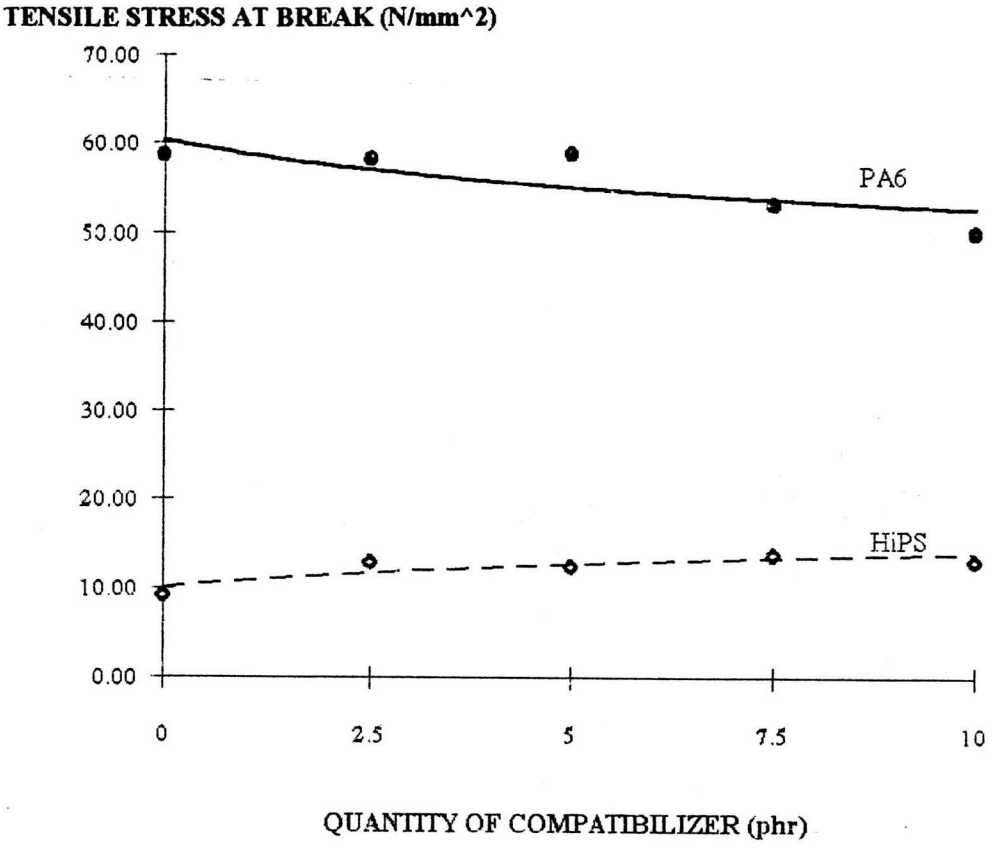

Figure 4.7: The tensile stress at break of compatibilized PA6 and HiPS plotted against the SEBS-g-MA concentrations.

As shown in Figure 4.7 the tensile stress at break of HiPS with SEBS-g-MA are higher than that of the pure HiPS. For PA6, the tensile stress at break has not changed significantly over the applied range of 0-5 phr of SEBS-g-MA . But beyond 5 phr, the tensile stress at break decreases sharply.

For HiPS, with 2.5, 5, 7.5 and 10 phr of SEBS-g-MA, the tensile stress at break increases by 40.9, 36.1, 50.5 and 41.8%. For PA6, with 2.5 and 5 phr of SEBS-g-MA, the tensile stresses at break remain unchanged. When the amount of SEBS-g-MA is increased to 7.5 and 10 phr, the tensile stress at break is found to be lower. At 7.5 and 10 phr of SEBS-g-MA, the tensile stress at break decreases by 9.2 and 14.7%.

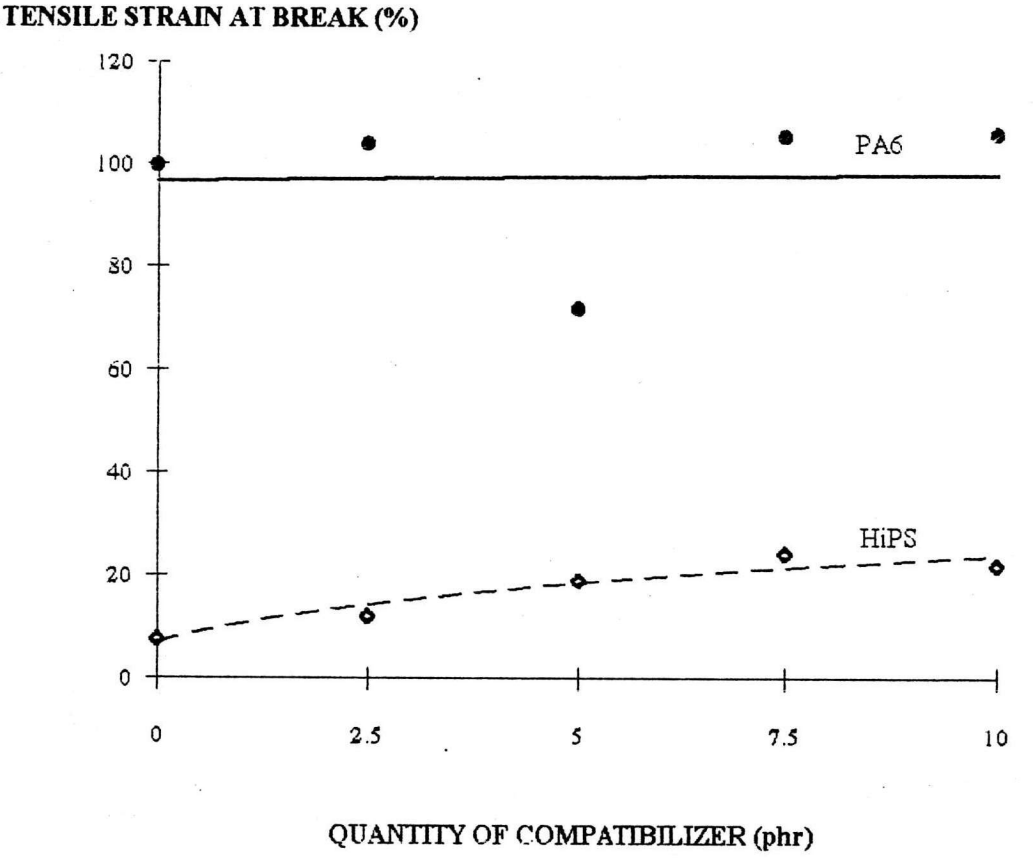

Figure 4.8: The tensile strain at break of compatibilized PA6 and HiPS plotted against the SEBS-g-MA concentrations.

The tensile strain at break of HiPS and PA6 is plotted against the amount of SEBS-g-MA in Figure 4.8. For HiPS, like the tensile stress at break, all the tensile strain at break of HiPS are greater than that of the pure HiPS. For PA6, most results depict an increasing trend from pure PA6.

For HiPS, with 2.5, 5, 7.5 and 10 phr of SEBS-g-MA, the tensile strain at break increases by 57.5, 149, 218.4 and 188.5%. For PA6, with 2.5, 7.5 and 10 phr of SEBS-g-MA, the tensile strain at break increases by 4.3, 5.7 and 6.2%.

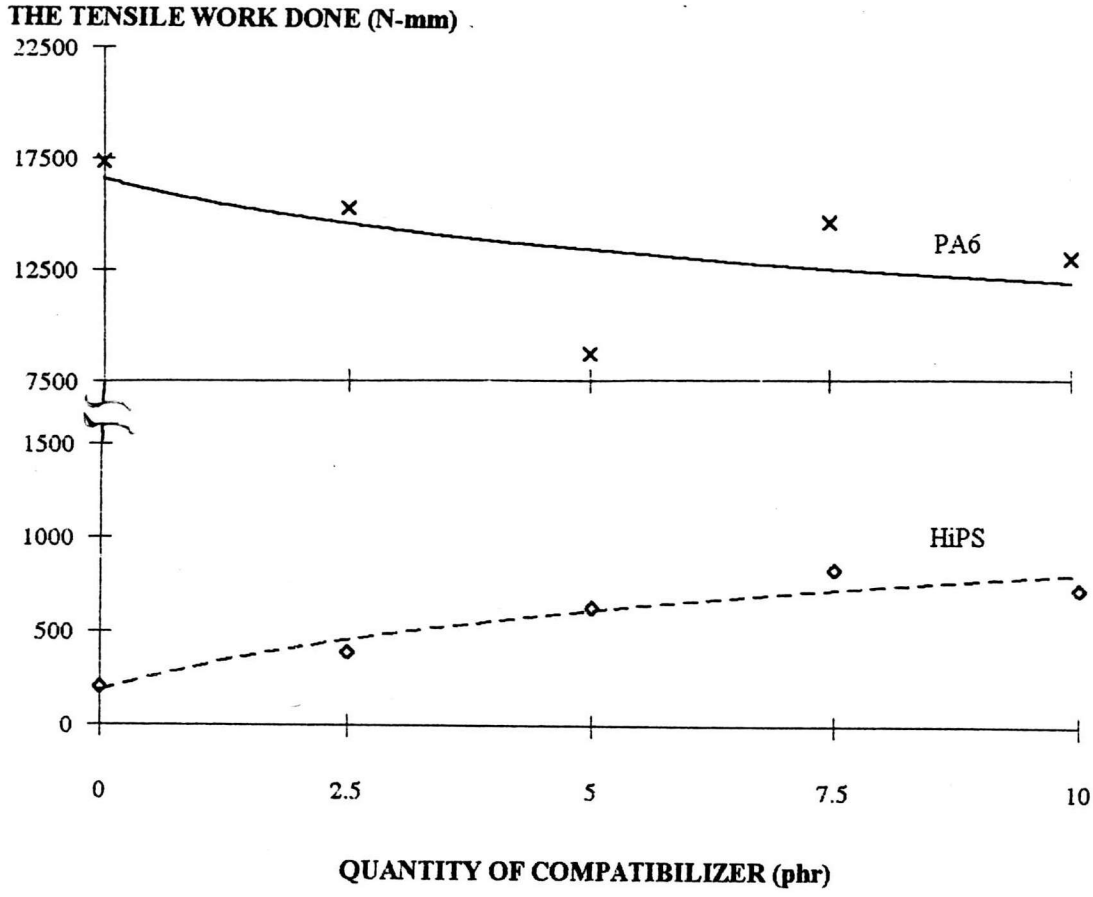

Figure 4.9: The tensile work done of compatibilized PA6 and HiPS plotted against the SEBS-g-MA concentrations.

As shown in Figure 4.9, all the tensile work done of HiPS with SEBS-g-MA are higher than that of the pure HiPS. The increase is gradual over the applied range from 0 to7.5 phr of SEBS-g-MA. Beyond 7.5 phr, there seens to be a minute increase at 10 phr of SEBS-g-MA. For PA6, all the tensile work done of PA6 with SEBS-g-MA are lower than that of the pure PA6.

For HiPS, when 2.5, 5, 7.5 and 10 phr of SEBS-g-MA was added, the tensile work done is elevated. The increase is found to be 91.8, 213.5, 318.2 and 265.1% respectively. For PA6, when 2.5, 5, 7.5 and 10 phr of SEBS-g-MA was added, the tensile work done is reduced. The reduction is found to be 12.2, 49.9, 16.2 and 25.7% respectively.

Hence it is apparent that when SEBS-g-MA is added to each parent polymer individually, there is significant change in the tensile properties as the following discussion:-

For tensile elastic modulus: the tensile elastic modulus of the multiphased polymer is lower than that of the matrix polymer when the second-phase particle is rubbery[17]. The addition of SEBS-g-MA in HiPS decreases the tensile elastic modulus of HiPS because SEBS-g-MA is thermoplastic rubber.

For PA6: At high concentration of SEBS-g-MA, i.e. 7.5 and 10 phr, the same explanation is applied. At low concentration, at 2.5 and 5.0 phr, grafting of MA-group on amine group on PA6 may have taken place. Consequently, the grafting reduces the movement of the PA6 chains. Thus, the tensile elastic modulus of PA6 is increased the effect of rubber phase to the elastic modulus is insignificant.

For 0.2% offset tensile yield stress: the 0.2% offset tensile yield stress of HiPS decreases when the amount of the SEBS-g-MA increases. Although the interface adhesion between the HiPS and the SEBS-g-MA is good, the SEBS-g-MA chain is easier to be stretched. As a consequence, the 0.2% offset tensile yield stress HiPS is reduced as more SEBS-g-MA is added.

For PA6: the 0.2% offset yield tensile stress increases as more SEBS-g-MA is added. This is believed to be due to the grafting effect induced by the SEBS-g-MA. The grafting between PA6 and SEBS-g-MA chains prevent the bond stretching of the chains. Hence, the 0.2% offset tensile yield stress of PA6 is greater with more SEBS-g-MA.

For the 0.2% offset tensile yield strain: Both the HiPS and the PA6 show a decreasing trend when more SEBS-g-MA is applied. These result from the dispersed SEBS-g-MA which lower 0.2% offset yield tensile strain in both the HiPS and the PA6.

For HiPS at break point, the addition of SEBS-g-MA enhances the opportunity for multiple crazing to take place. The SEBS-g-MA act as the craze initiating site. The more the amount of the SEBS-g-MA , the greater the craze initiating points as well as craze termination points. So, the tensile stress and the tensile strain at break as well as the tensile work done of HiPS tends to increase with the SEBS-g-MA concentrations.

For PA6: According to the model of O. K. Muratoglu *et al.* [18] as shown in Figure 4.10, the yield stress should be lowered in regions of easy shear. This local softening phenomenon should reduce the overall flow stress of the material, allowing it to deform to large tensile strain without initiating any critical fracture process. Thus, the toughness is increased. Hence, the tensile stress at break is decreased while the tensile strain at break is increased.

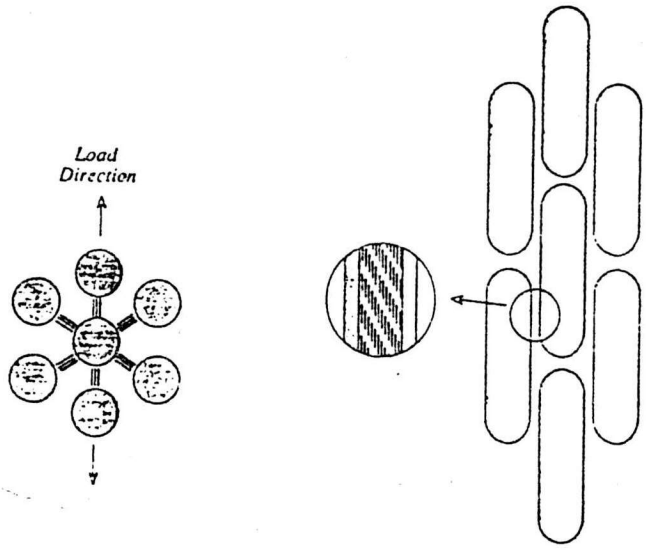

Figure 4.10: Schematic diagram for the deformation mechanism of an idealized morphology under uniaxial tensile test: (a) before and (b) after deformation. In (a) the parallel lines represent the intersection of lamellae with the plane of the paper while in (b) the line enlarged region represent that of the hydrogen-bonded planes.

The overall tensile work done is reduced because the tensile strain at break increases only a little while the tensile stress at break decreases drastically and rapidly.

4.2.1.2 Izod impact strength

The test is particularly useful in assuring the energy required to break a notched specimen. The high value of the Izod impact strength is an indication of the more impact resistance the material is.

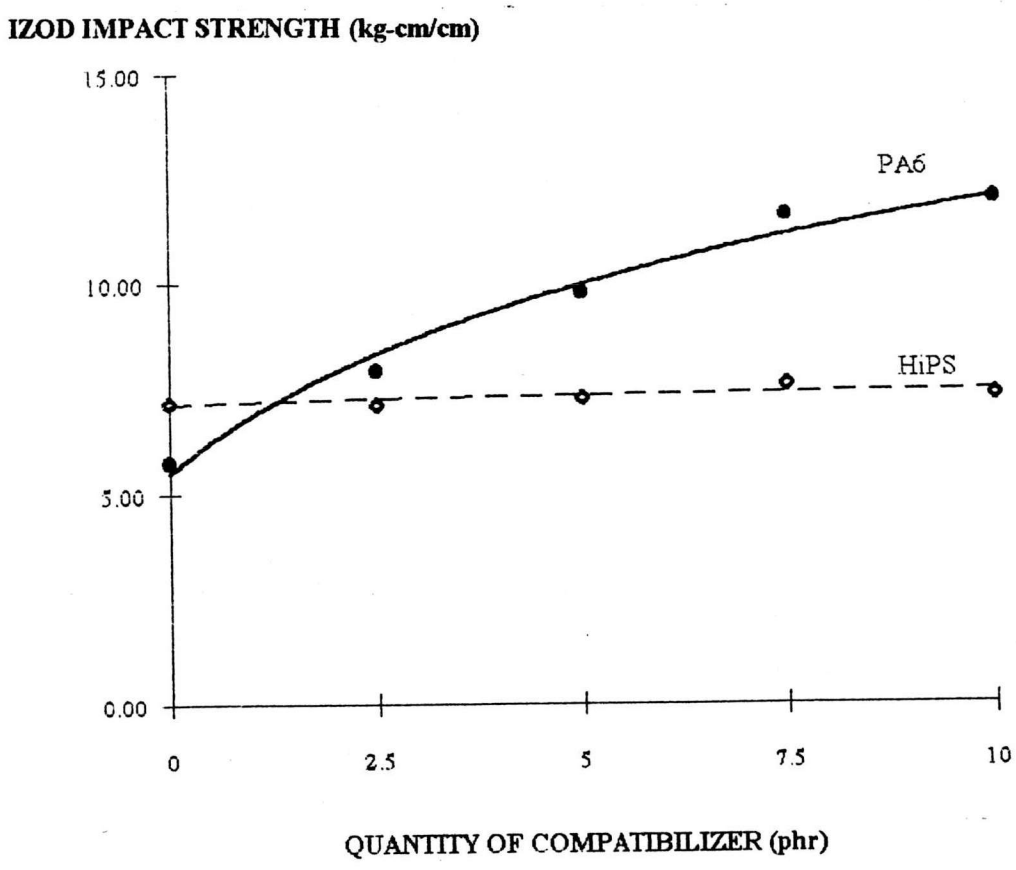

Figure 4.11: The Izod impact strength of compatibilized PA6 and HiPS plotted against the SEBS-g-MA concentrations.

Figure 4.11 is a plot of the Izod impact strength against the concentrations of SEBS-g-MA. The addition of SEBS-g-MA has no effect on the Izod impact strengthto HiPS . On the other hand, it exhibits significantly increase in the Izod impact strength of PA6. An addition of the SEBS-g-MA by 2.5, 5, 7.5 and 10 phr leads to an increase in the Izod impact strength of PA6 by 37.7, 69.6, 101.4 and 108%.

The rubber phase can blunt the crack tip. Based on the model showwn in Figure 4.10, the crack tip in PA6 may have propagated into the high strength ligament between the particles or the crack is blunted by the rubber phase. Hence, the Izod impact strength of PA6 is increased with the SEBS-g-MA concentrations.

4.2.1.3 Falling-weight test.

In addition to the energy to break a plate material, there is test that takes into account the frictional 'push-through' energy term. The test is known as the falling weight test.

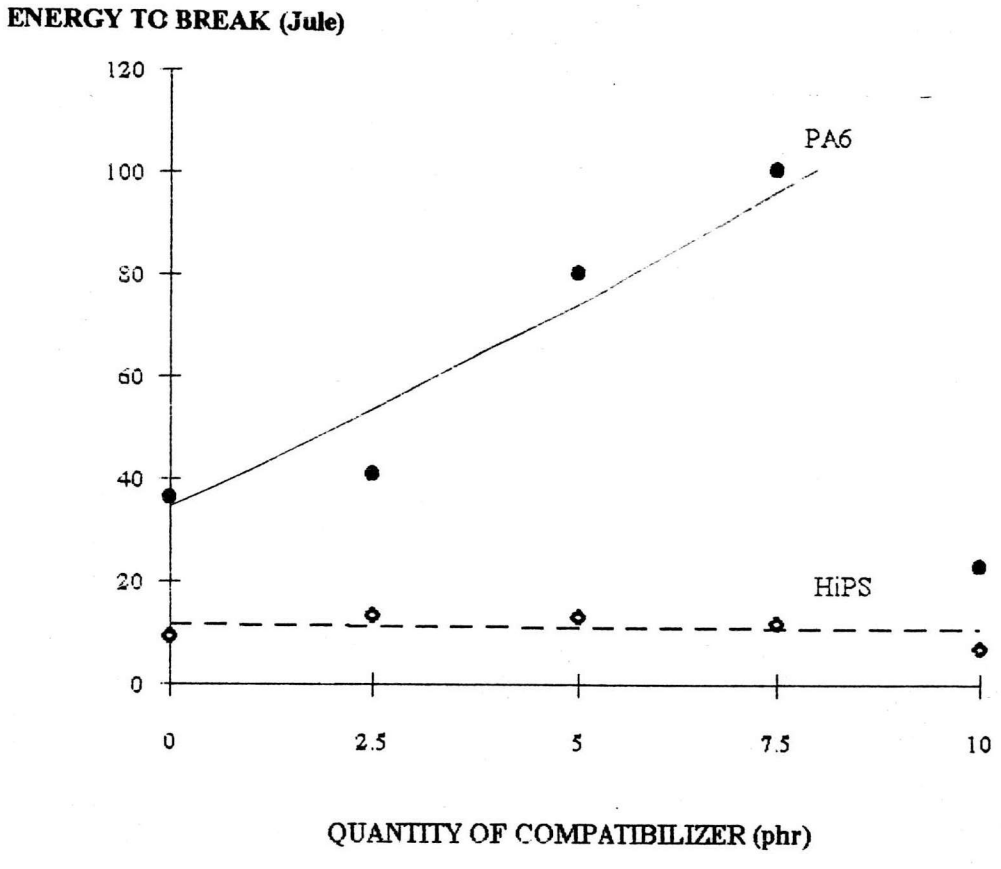

Figure 4.12: The falling-weight impact energy of compatibilized PA6 and HiPS plotted against the SEBS-g-MA concentrations.

As shown in Figure 4.12, the falling-weight impact energy of PA6 increases suddenly over the applied range of 0 to 7.5 phr of SEBS-g-MA. But at 10 phr the falling-weight impact energy decrease sharply. For HiPS, the falling-weight impact energy increases slightly at 2.5 and 5

phr of SEBS-g-MA. Overall the SEBS-g-MA seems to have no significant effect on the falling-weight impact energy of HiPS.

For PA6, when 2.5-7.5 phr of SEBS-g-MA was added, the falling-weight impact energy increases by 12.3, 120.1 and 175.9% but when 10 phr of SEBS-g-MA was added the falling weight impact energy decrease by 36.8%. This unexpected decreasing may come from error in testing.

The falling weight energy to break of HiPS increases by the increasing of multiple crazing and more deformation. For PA6, the falling weight energy to break increases by the existing of ligament between particle and more deformation.

4.2.1.4 Heat-distortion temperature (HDT)

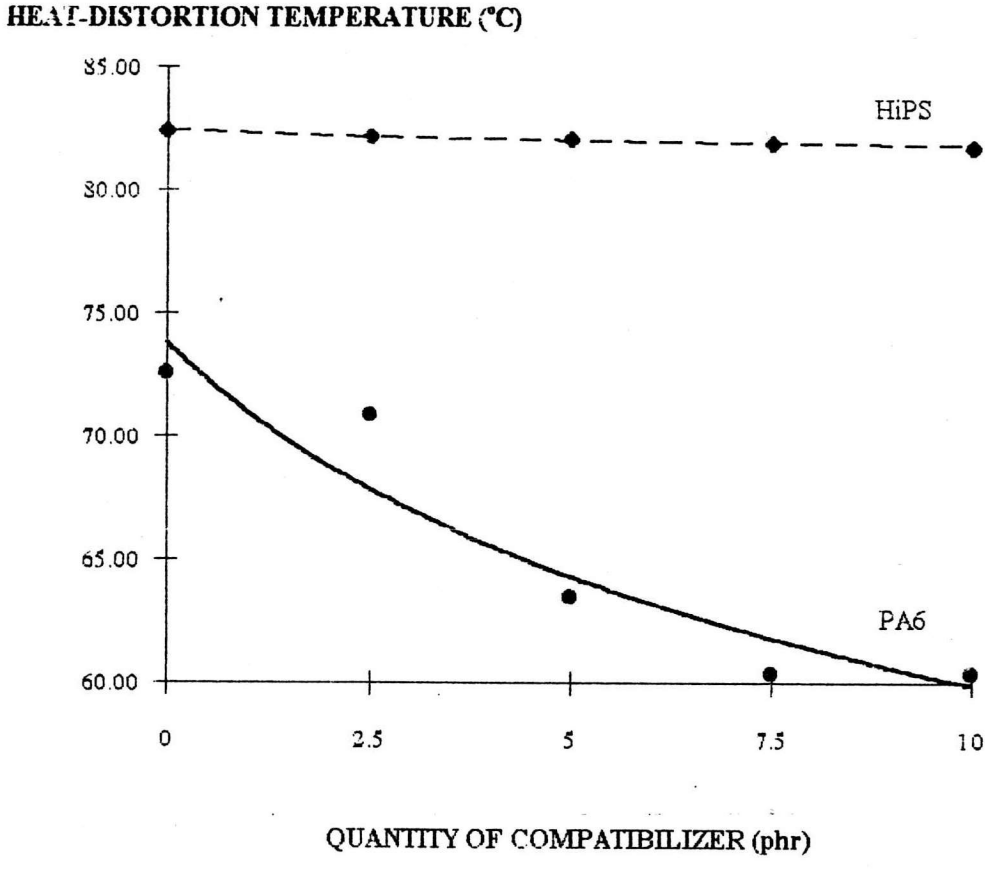

Figure 4.13: The heat distortion temperature of compatibilized PA6 and HiPS plotted against the SEBS-g-MA concentrations.

From Figure 4.13, it is clear that the HDT of HiPS decrease very slightly when SEBS-g-MA is added. The HDT of PA6 decreases significantly as the SEBS-g-MA concentration is increased. For PA6, with 2.5, 5, 7.5 and 10 phr of SEBS-g-MA, the HDT decreases by 2.3, 12.5, 16.8 and 16.8%.

The HDT of both PA6 and HiPS decrease because adding rubber phase (SEBS-g-MA) which has lower glass transition temperature.

4.2.2 PA6/HiPS blends

4.2.2.1 Tensile properties

The mechanical properties in terms of the stress-strain of the PA6, HiPS and uncompatibilized PA6/HiPS blends were obtained and shown as the load-deformation plot in Figure 4.14. The plots show that PA6/HiPS blends at 80/20, 60/40 and 40/60 exhibit the load-deformation curves to be similar in pattern to that of pure PA6. The only difference is that the load and deformation involved were much lower when PA6 was reduced. The 20/80 composition of PA6/HiPS blend behaves closer to that exhibited by HiPS. A distinct extrinsic yield point is observed in both the pure HiPS and the 20/80 PA6/HiPS blend. In addition the energy required to fracture the blends in tension decreases as the PA6 constituent is reduced. The 20/80 composition of PA6/HiPS blend requires less energy to break the blend than that for the pure HiPS.

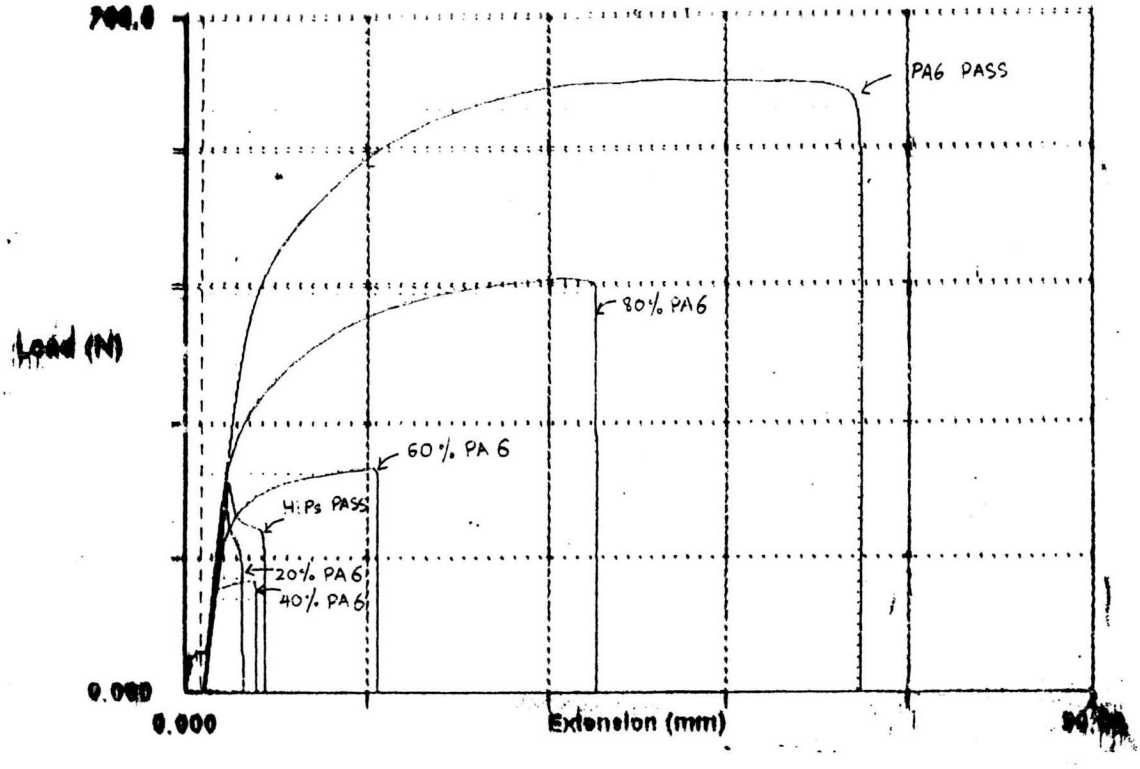

Figure 4.14: The load-deformation diagram from tensile test of PA6, HiPS and uncompatibilized PA6/HiPS blends.

When SEBS-g-MA was added to the PA6 HiPS and PA6/HiPS blends. The mechanical properties in terms of the stress-strain of the PA6, HiPS and compatibilized PA6/HiPS blends were obtained and shown as the load-deformation plot in Figure 4.15. The plots show that compatibilized PA6/HiPS blends exhibit the load-deformation curves to be similar in pattern to that of uncompatibilized PA6/HiPS blends in Figure 4.14. But the energy required to fracture the compatibilized blends in tension increases from the uncompatibilized blends.

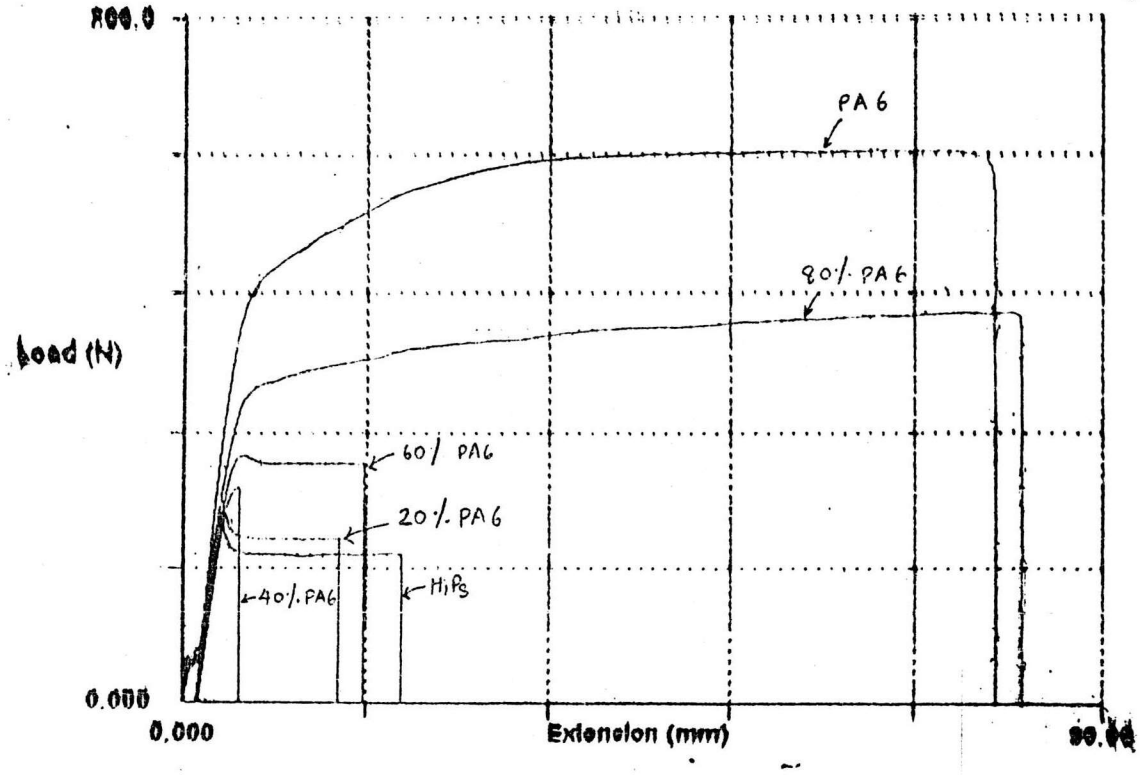

Figure 4.15: The load-deformation diagram from tensile test of PA6, HiPS and compatibilized PA6/HiPS blends.

The tensile elastic modulus is estimated and plotted against the amount of the PA6 constituent for the various blend formulations are compared in Figure 4.16

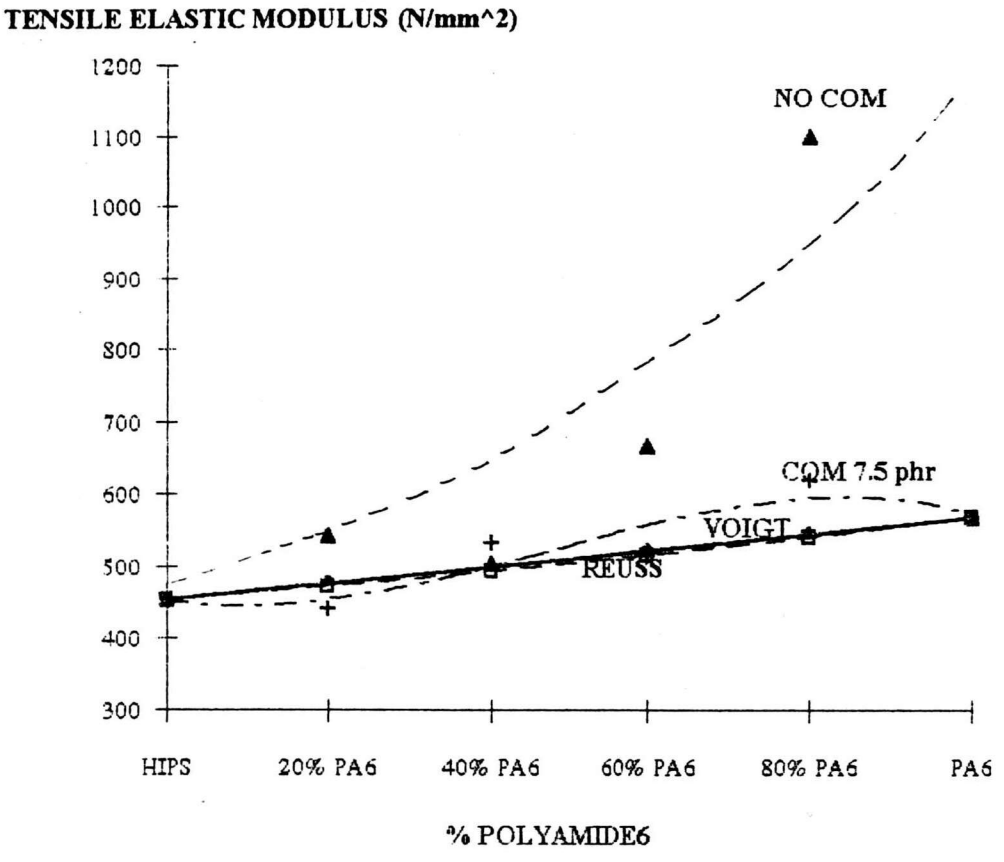

Figure 4.16: The tensile elastic modulus of uncompatibilized and compatibilized PA6/HiPS blends plotted against the PA6 concentrations.

The theoretical elastic modulus estimated by Voigt's and Reuss' models are shown in the piot. The actual modulus of elasticity obtained in the uncompatibilized PA6/HiPS blends shows a rapid increase initially as the PA6 content becomes greater. It is clear that the tensile elastic modulus of the blends are grater than those estimated by Voigt's and Reuss' model at all concentrations.

With the presence of the 7.5 phr compatibilizer, the modulus of elasticity is drastically lowered by approximately 20 %. The reduction of the modulus of elasticity is believed to be the lubricant effect induced by the compatibilizer, which reacts with both the PA6 and HiPS. When polymer chains are stretched, chain mobility takes place and it is enhanced by the cooperative movement of both the PA6 chains, the HiPS chains and the compatibilizer at the interface linking the two polymers.

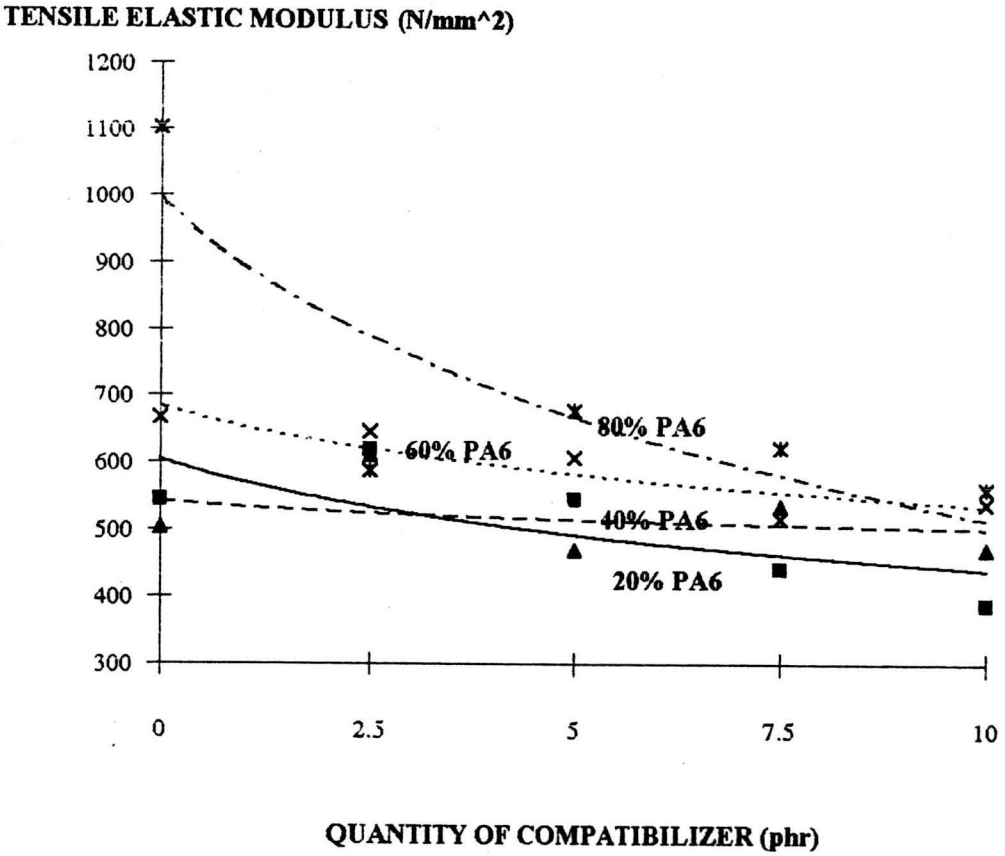

Figure 4.17: The tensile elastic modulus of compatibilized PA6/HiPS blends plotted against the SEBS-g-MA concentrations.

From Figure 4.17, it shows that the tensile elastic modulus of 80/20 PA6/HiPS blend decreases sharply from 0 to 2.5 phr of SEBS-g-MA. But the tensile elastic modulus insignificantly change beyond 2.5 phr of the SEBS-g-MA. While the tensile elastic modulus of 60/40 and 20/80 PA6/HiPS blends decrease gently when the quantity of compatibilizer increase. Additional the tensile elastic modulus of 40/60 PA6/HiPS blend seem to have unchanged trend.

For 80/20 PA6/HiPS blend, when 2.5 to 10 phr. of the SEBS-g-MA was added the tensile elastic modulus is felled. At 2.5, 5, 7.5 and 10 phr of the SEBS-g-MA, the tensile elastic modulus decreases by 46.6, 38.5, 43.6 and 49.2%. For 60/40 PA6/HiPS blend, when 2.5 to 10 phr of the SEBS-g-MA was added, the tensile elastic modulus is reduced. At 2.5, 5, 7.5 and 10 phr of the SEBS-g-MA, the tensile elastic modulus decreases by 3.1, 9, 22.7 and 19.1%. For 20/80 PA6/HiPS blend, when 2.5 to 5 phr of the SEBS-g-MA was added, the tensile elastic modulus is elevated. Above 5 phr of the SEBS-g-MA is felled. At 2.5, 5, 7.5 and 10 phr of SEBS-g-MA, the tensile elastic modulus change by 13.8, 0.2, -18.9 and -28.8% .

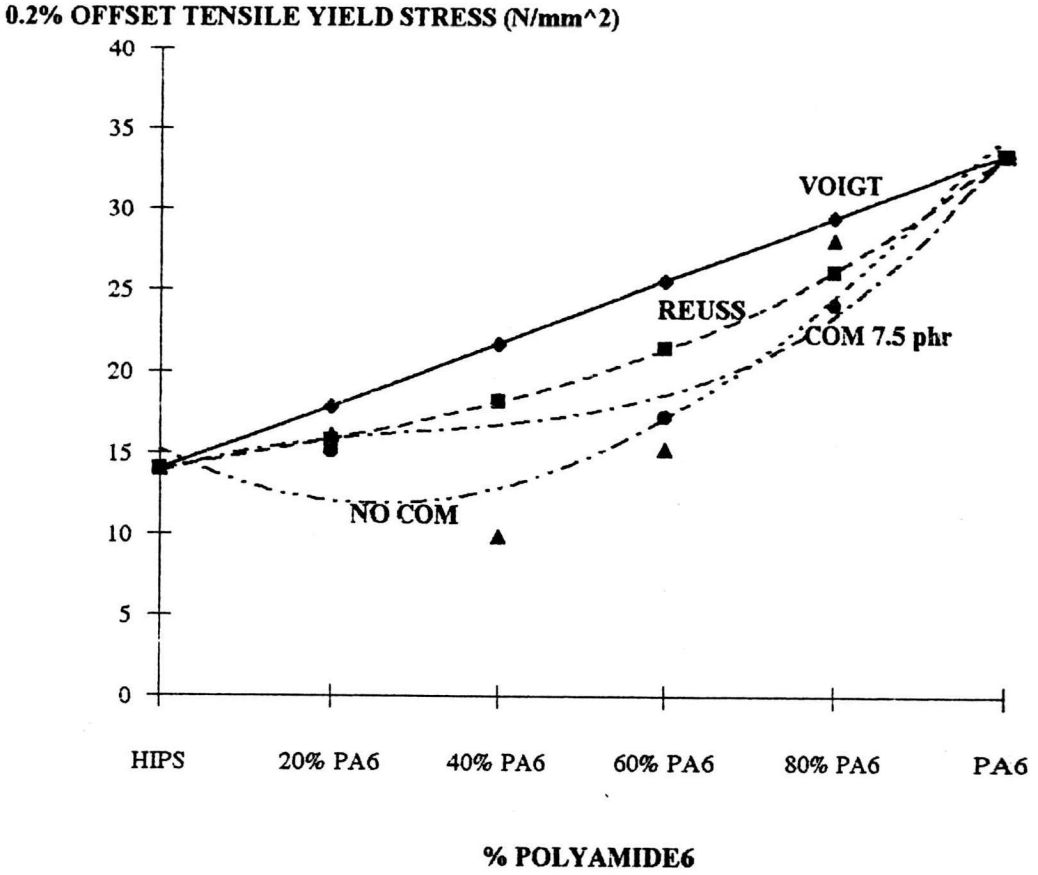

Figure 4.18: The 0.2% offset tensile yield stress of PA6/HiPS blends with and without compatibilizer plotted against the PA6 concentrations.

Figure 4.18 shows that the 0.2% offset tensile yield stress plotted against the PA6 content in the blends. In uncompatibilized blends the 0.2% offset tensile yield stress for the both the 40/60 and 60/40 PA6/HiPS blends are lower than those estimated by Voigt's model and the Reuss' model. While those of the 20/80 and 80/20 PA6/HiPS blends are only slightly lower than the value estimated by Voigt's model and slightly higher than that based on Reuss' model.

With the presence of the 7.5 phr compatibilizer, the 0.2% offset tensile yield stress is slightly lowered by approximately 10 % for 20/80 and 80/20 PA6/HiPS blends. This reduction in the 0.2% offset tensile yield stress is believed to be the presence of compatibilizer in the matrix of these blends. Because the bond stretching of SEBS-g-MA chain is low, when polymer chains are stretched, the SEBS-g-MA chain is previously stretched. Whereas it is highered approximately 40 % for 40/60 and 60/40 PA6/HiPS blends. This increasing in the 0.2% offset tensile yield stress is believed to be the continuty of the blends effect. The addition of compatibilizer enhance the dispersion and distribution of domain and interface adheresion. So the amount of matrix polymer chains is increased. These cause the increasing of continuity of matrix phase and interface of two polymers, so that the 0.2% offset yield tensile stress are increased.

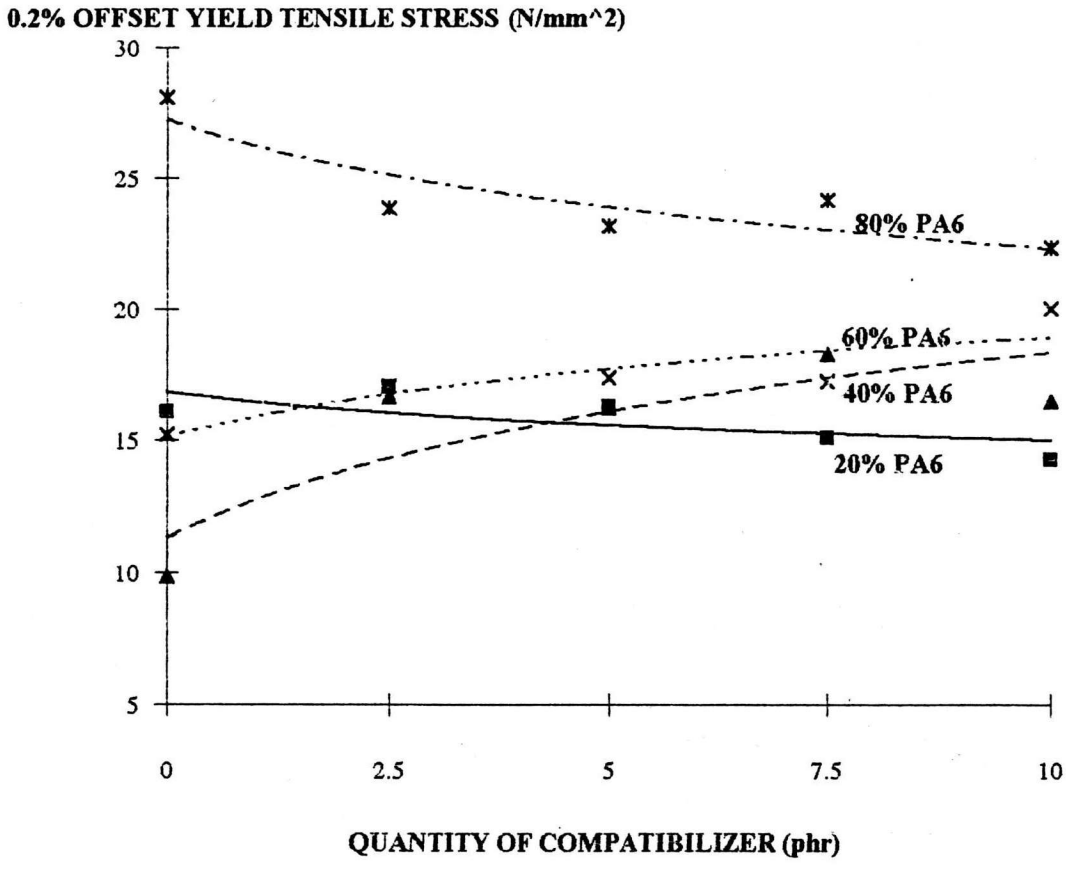

Figure 4.19: The 0.2% offset tensile yield stress of compatibilized PA6/HiPS blends plotted against SEBS-g-MA concentrations.

For more compatibilizer content, some composition decrease and some composition increase but this changes are less than 20% from compatibilizer 2.5 phr to 10 phr.

As shown in Figure 4.19, it shows that the 0.2% offset tensile yield stress of 80/20 and 20/80 PA6/HiPS blends decrease when amount of compatibilizer increase. Whereas the 0.2% offset tensile yield stress of 60/40 and 40/60 PA6/HiPS blends increase when amount of compatibilizer increase.

For 80/20 PA6/HiPS blend, with 2.5, 5, 7.5 and 10 phr of SEBS-g-MA, the 0.2% offset tensile yield stress decrease by 15.1, 17.6, 14.1 and 20.5%. For 60/40 PA6/HiPS blend, with 2.5, 5, 7.5 and 10 phr of SEBS-g-MA, the 0.2% offset yield tensile stress increases by 12.2, 14.3, 13.3 and 31.4%. For 40/60 PA6/HiPS blend, with 2.5, 5, 7.5 and 10 phr of SEBS-g-MA, the 0.2% offset yield tensile stress increases by 69.2, 65, 85.6 and 67.4%. For 20/80 PA6/HiPS blend, with 2.5 and 5 phr of SEBS-g-MA, the 0.2% offset tensile yield stress increases by 5.8 and 1.2% but with 7.5 and 10 phr of SEBS-g-MA, the 0.2% offset tensile yield stress decreases by 6.2 and 11.3%

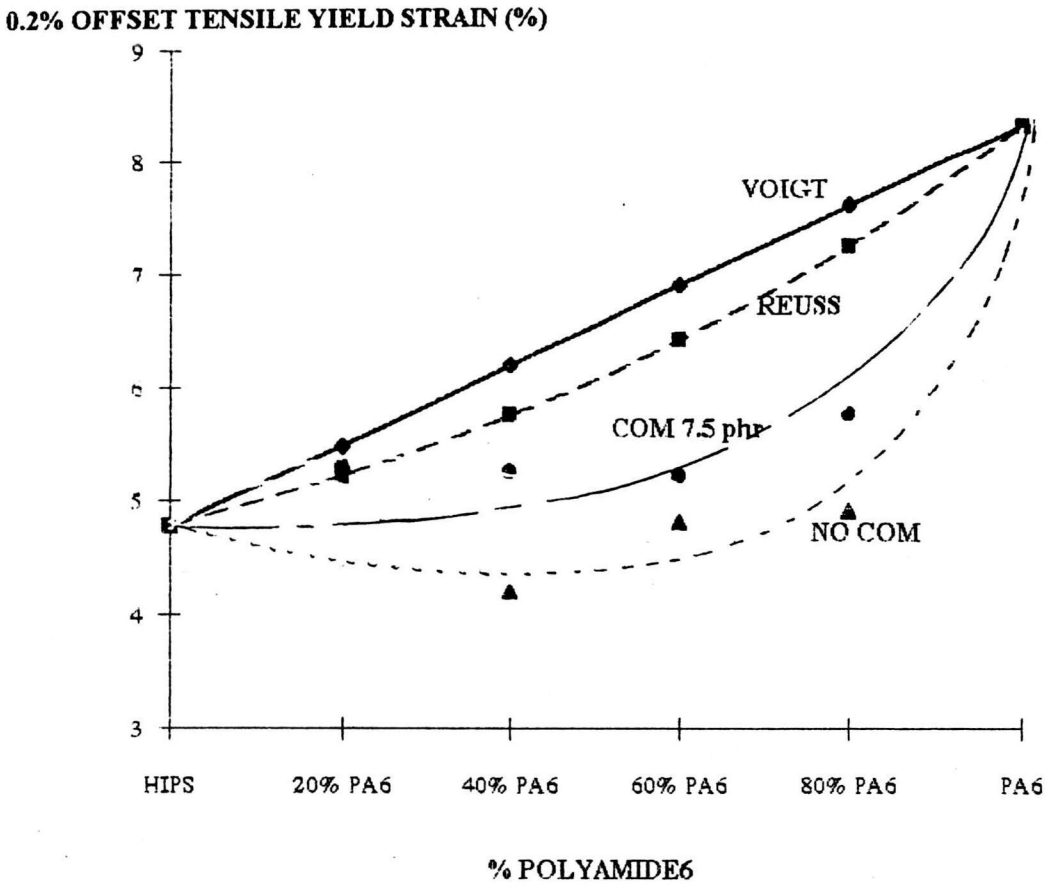

Figure 4.20: The 0.2% offset tensile yield strain of PA6/HiPS blends with and without compatibilizer plotted against the PA6 concentrations.

Figure 4.20 shows that the actual 0.2% offset tensile yield strain in the uncompatibilized PA6/HiPS blends fell from 5.20 % strain for one-passed HiPS to 4.21% strain for 40/60 PA6/HiPS blend and it rise gradually to 6.20% for one process PA6. It is clear that the most 0.2% offset tensile yield strain of the blends are lower than the estimated by Voigt's and Reuss' models.

With the presence of the 7.5 phr compatibilizer, the 0.2% offset tensile yield strain is slightly highered by approximately 15 %. This increasing in the 0.2% offset yield tensile strain is believed to be the presence of compatibilizer in the matrix of 20/80 and 80/20 PA6/HiPS blends and the continuity of blends effect in 40/60 and 60/40 PA6/HiPS blends, similar the 0.2% offset tensile yield stress.

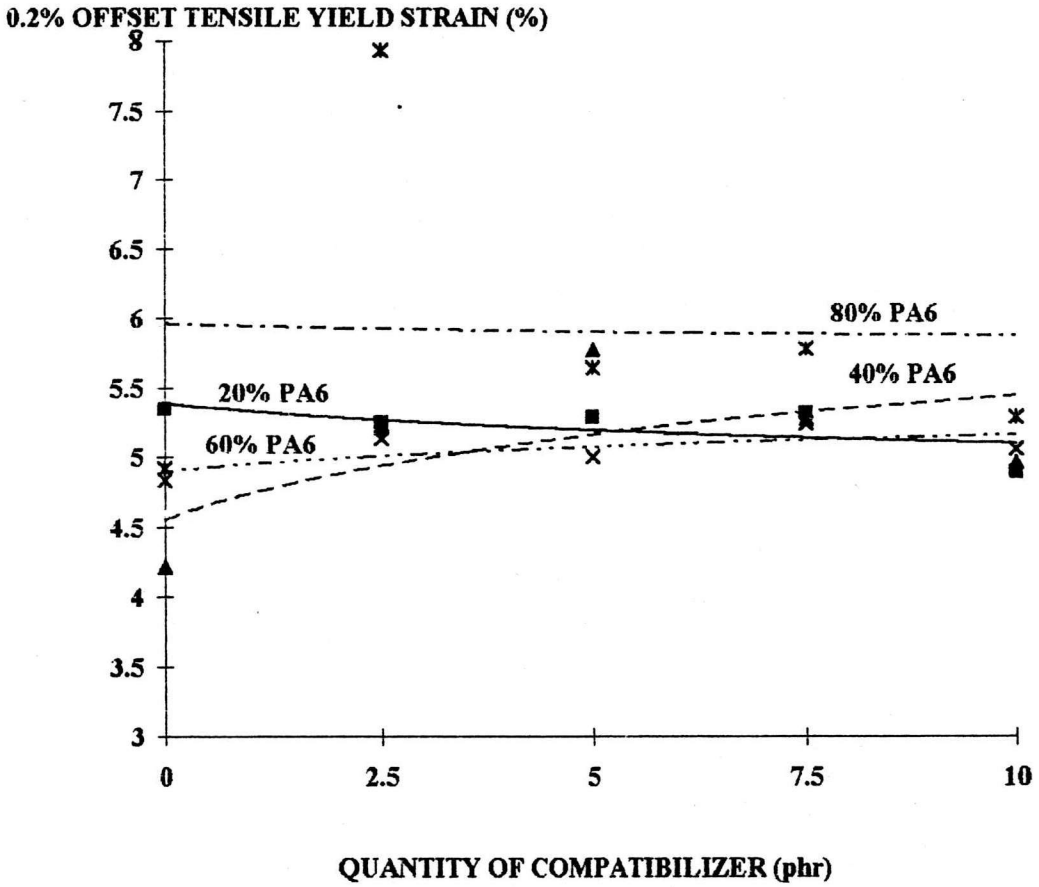

Figure 4.21: The 0.2% offset tensile yield strain of compatibilized PA6/HiPS blends plotted against the SEBS-g-MA concentrations.

Addition of compatibilizer increases all the 0.2% offset tensile yield strain from uncompatibilized blends. But the more compatibilizer content increases, the more strain at offset yield decreases. Significantly at 80/20 PA6/HiPS, the 0.2% offset tensile yield strain decreases about 28% from 2.5 phr to 5.0 phr compatibilizer content.

As shown in Figure 4.21, all the 0.2% offset tensile yield strain of 80/20, 60/40 and 40/60 PA6/HiPS blends with SEBS-g-MA are higher than that of the uncompatibilized blends. Whereas all the 0.2% offset tensile yield strain of 20/80 PA6/HiPS blend with SEBS-g-MA are lower than that of the uncompatibilized blend.

For 80/20 PA6/HiPS blend, with 2.5, 5, 7.5 and 10 phr of the SEBS-g-MA, the 0.2% offset tensile yield strain increases by 61.4, 41.6, 17.5 and 7.9%. For 60/40 PA6/HiPS blend, with 2.5, 5, 7.5 and 10 phr of the SEBS-g-MA, the 0.2% offset tensile yield strain increases by 6.3, 3.6, 8.4 and 4.7%. For 40/60 PA6/HiPS blend, with 2.5, 5, 7.5 and 10 phr of the SEBS-g-MA, the 0.2% offset tensile yield strain increases by 23.6, 36.9, 25 and 17.6%. For 20/80 PA6/HiPS blend, with 2.5, 5, 7.5 and 10 phr of the SEBS-g-MA, the 0.2% offset tensile yield strain increases by 2, 1.1, 0.6 and 8.5%.

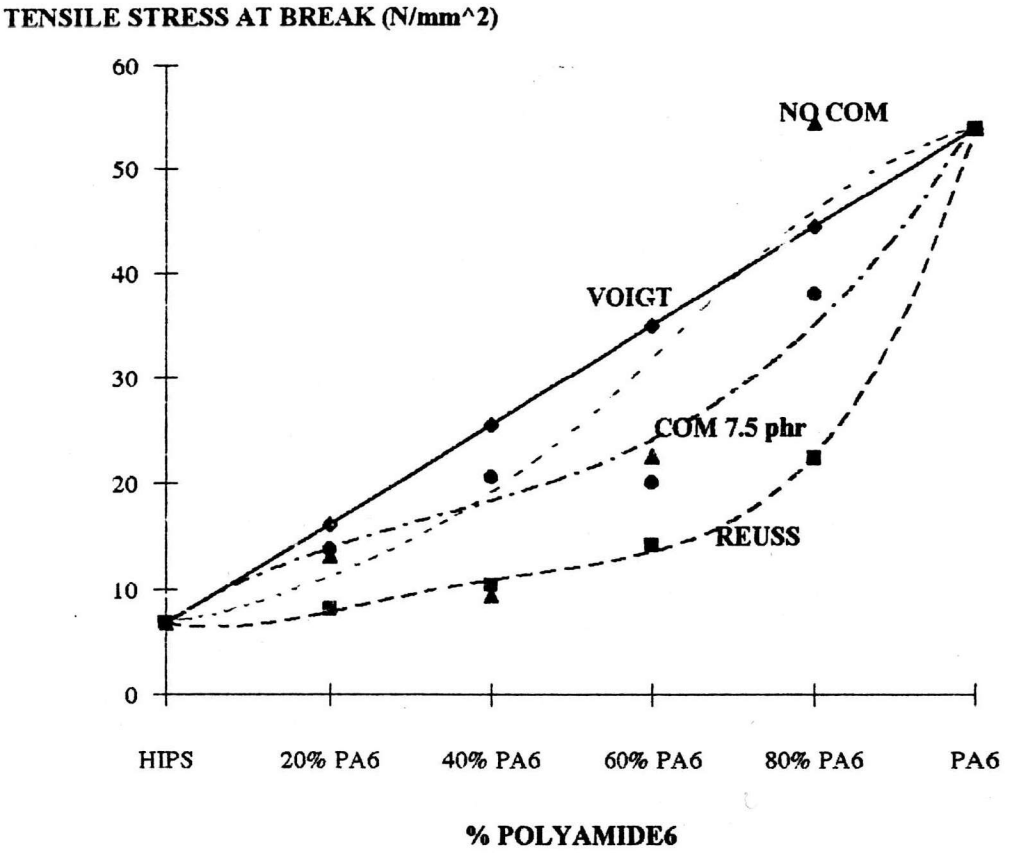

Figure 4.22: The tensile stress at break of uncompatibilized and compatibilized PA6/HiPS blends plotted against the PA6 concentrations.

Figure 4.22 shows that the uncompatibilized blends pass the tensile stress at break at the level between Voigt and Reuss' model for the one-passed HiPS to the 60/40 PA6/HiPS blend. Then the actual tensile stress at break rises over the values estimated based on both the Voigt and the Reuss' law. At 80/20 PA6/HiPS blends the tensile stress at break is significantly 22% higher than predicted by Voigt's model.

With the presence of the 7.5 phr compatibilizer, the tensile stress at break is highered for 20/80 and 40/60 PA6/HiPS blends, HiPS is the matrix. The increasing in the tensile stress at break is believed to be interface adhesion effect induced by the compatibilizer. Under tension the micromechanical deformation in HiPS is the crazes are formed. As a result of dispersed phase, there is a creation of new internal surfaces. During crazing, the domain particles are debonded or detached from matrix. The addition of SEBS-g-MA reduces domain size and increases interface adhesion. These results increase force to debond or detach the domain particles from matrix.

With the presence of the 7.5 phr compatibilizer, the tensile stress at break is highered for 60/40 and 80/20 PA6/HiPS blends, PA6 is the matrix. The reduction in the tensile stress at break is believed to be local softening phenomenon induced by the compatibilizer, the same as PA6 with SEBS-g-MA. Under tension, the micromechanical mechanism in PA6 is that shear bands are formed. As a result of dispersed phase, there are some cavitation at the surface of the matrix and the domain. The addition of SEBS-g-MA increases the dispersion of domain and interface adhesion. These results increase local softening phenomenon which decreases tensile stress at break.

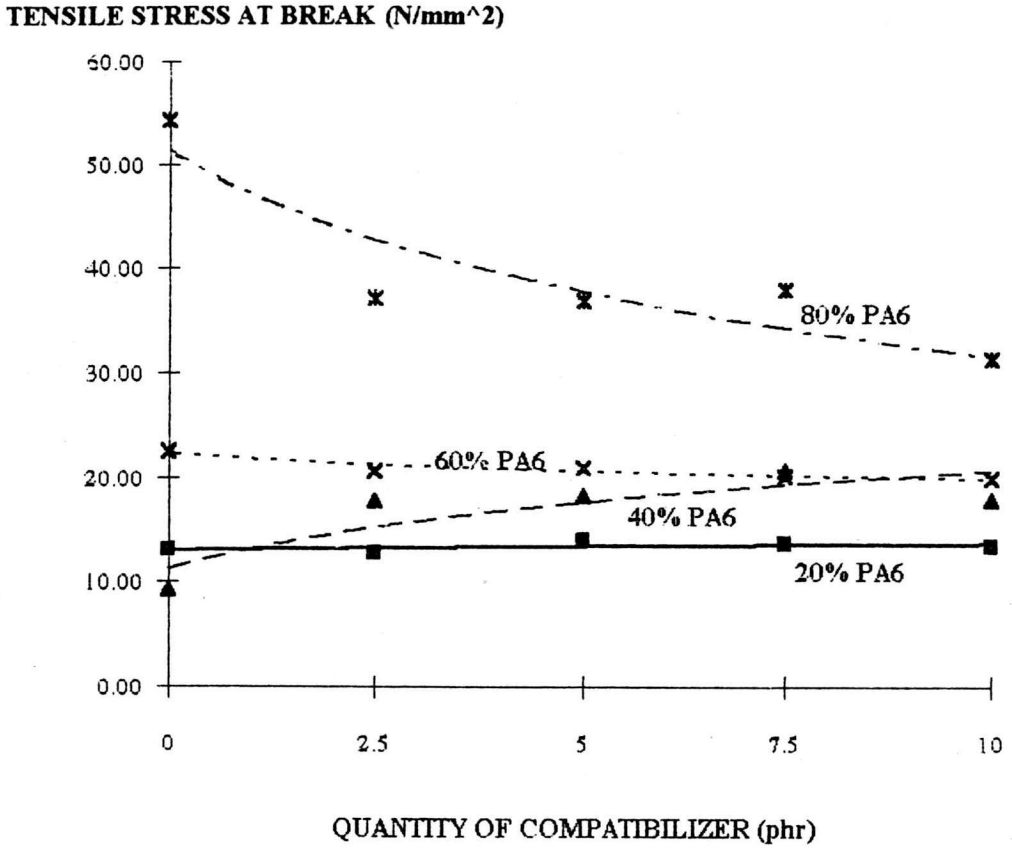

Figure 4.23: The tensile stress at break of compatibilized PA6/HiPS blends plotted against the SEBS-g-MA concentrations.

The tensile stress at break of PA6/HiPS blends is shown plotted against the amount of the SEBS-g-MA in Figure 4.23. For 80/20 PA6/HiPS blend, the tensile stress at break decreases sharply from 0 to 2.5 phr of SEBS-g-MA. But the tensile stress at break insignificantly decrease between 2.5-7.5 phr of SEBS-g-MA. For 60/40 PA6/HiPS blend, the tensile stress at break decreases a little when the quantity of SEBS-g-MA increases. For 40% PA6, all the tensile stress at break are higher than that of uncompatibilized 40/60 PA6/HiPS blend. For 20/80 PA6/HiPS blend, the tensile stress at break insignificantly change when the quantity of SEBS-g-MA increases.

For 80/20 PA6/HiPS blend, when 2.5-10 phr of SEBS-g-MA was added, the tensile stress at break decreases by 34.4, 31.9, 30.1 and 42.3%. For 60/40 PA6/HiPS blend, when 2.5-10 phr of SEBS-g-MA was added, the tensile stress at break decreases by 8.4, 7.3, 10.9 and 11.6%. For 40/60 PA6/HiPS blend, when 2.5-10 phr of SEBS-g-MA was added, the tensile stress at break significantly increases by 90.1, 95.4, 121.4 and 91.8%.

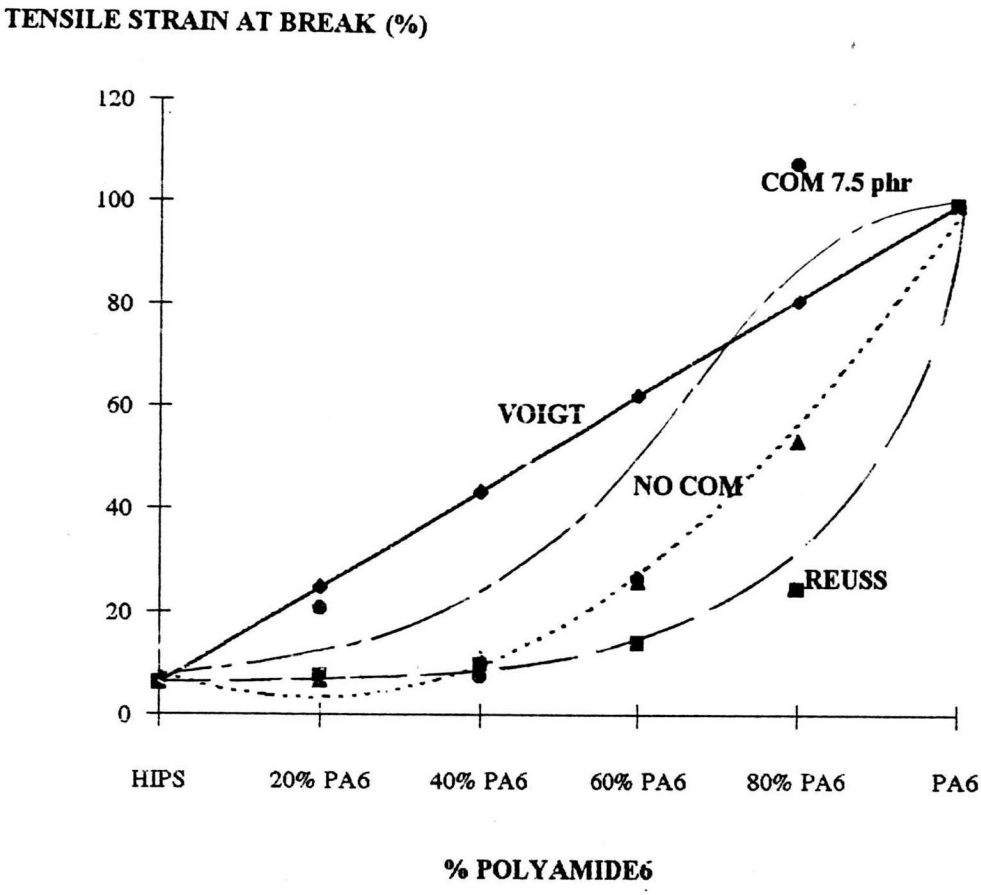

Figure 4.24: The tensile strain at break of uncompatibilized and compatibilized PA6/HiPS blends plotted against the PA6 concentrations.

The actual the tensile strain at break obtain in the uncompatibilized PA6/HiPS blends shows a rapid increase as the PA6 content becomes greaster. From Figure 4.8, the strain at break of uncompatibilized blends settles between those estimated by the Voigt and Reuss' model. An exception is for the 20/80 PA6/HiPS blend in which the strain at break is insignificantly lower than that based on Reuss' model. The tensile strain at break fell from 7.57% stain for one-passed

HiPS to 6.59% for 20/80 PA6/HiPS blend and it rise dramaticly to 99.77% stain for one-passed PA6.

With the presence of the 7.5 phr compatibilizer, the tensile strain at break is drastically highered. The increasing in the tensile strain at break is believed to be interface adhesion effect and local softening phenomenon induced by the compatibilizer, similar to the tensile stress at break. In HiPS matrix, 20/80 PA6/HiPS blends, the improvement of interface adhesion increase the tensile strain at break. But in 40/60 PA6/HiPS blends have inverse result from 20/80 PA6/HiPS blends. This result may effect from the reduce of domain aspect ratio induced by the compatibilizer. In PA6 matrix, 60/40 and 80/20 PA6/HiPS blends, The local softening phenomenon should reduce the overall flow stress of the material allowing it to deform to large tensile strain without initiating any critical fracture process.

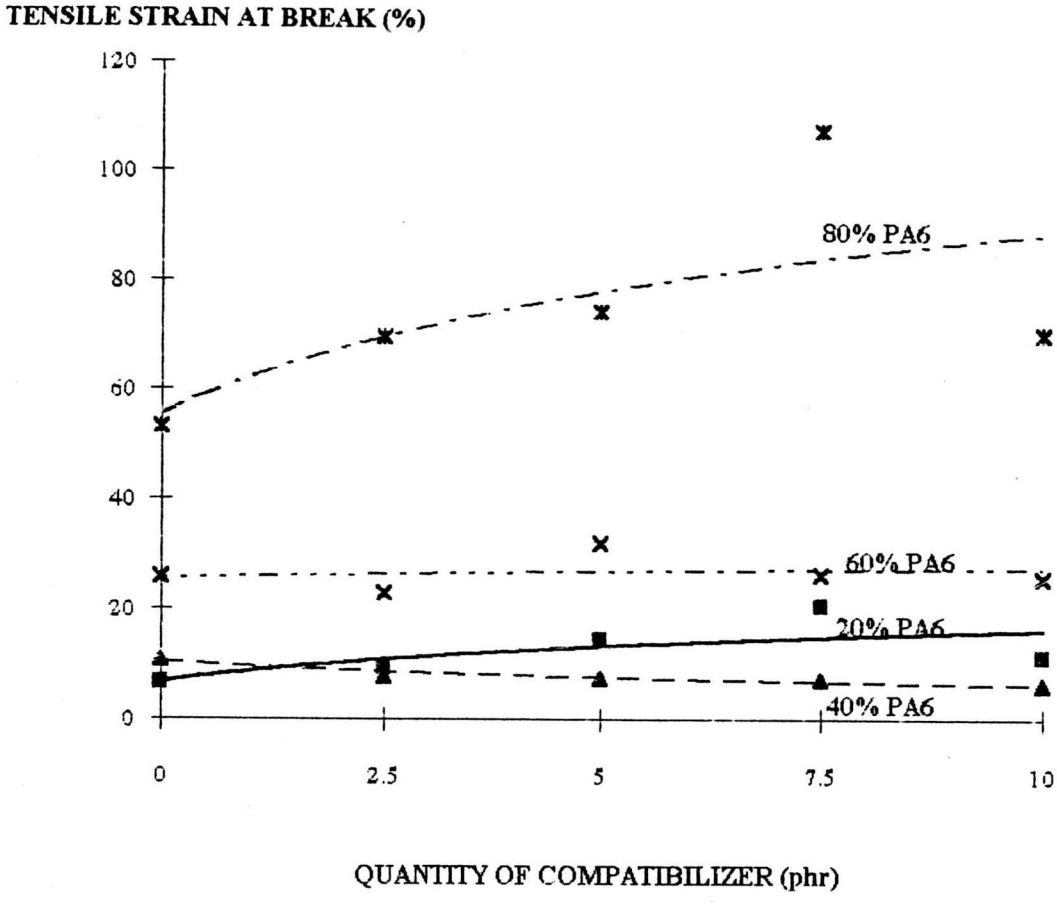

Figure 4.25: The tensile strain at break of compatibilized PA6/HiPS blends with SEBS-g-MA concentrations.

For Figure 4.25, it shows that the addition of SEBS-g-MA increases the tensile strain at break for 80/20 PA6/HiPS blends. For 60/40 PA6/HiPS blends, the tensile strain at break insignificantly changes when the amount of SEBS-g-MA increases. For 40/60 PA6/HiPS blends, the addition of SEBS-g-MA decreases the tensile strain at break. For 20/80 PA6/HiPS blends the tensile strain at break increases when the amount of compatibilizer increases.

For 80/20 PA6/HiPS blends, with 2.5, 5, 7.5 and 10 phr of SEBS-g-MA, the tensile strain at break increases by 31, 39.3, 101.7 and 31.8%. For 40/60 PA6/HiPS blends, with 2.5, 5, 7.5 and 10 phr of SEBS-g-MA, the tensile strain at break decreases by 27.8, 32.2, 33.2 and 42.1%. For 20/80 PA6/HiPS blends, with 2.5, 5, 7.5 and 10 phr of SEBS-g-MA, the tensile strain at break increases by 42.9, 119.6, 211.9 and 72.9%.

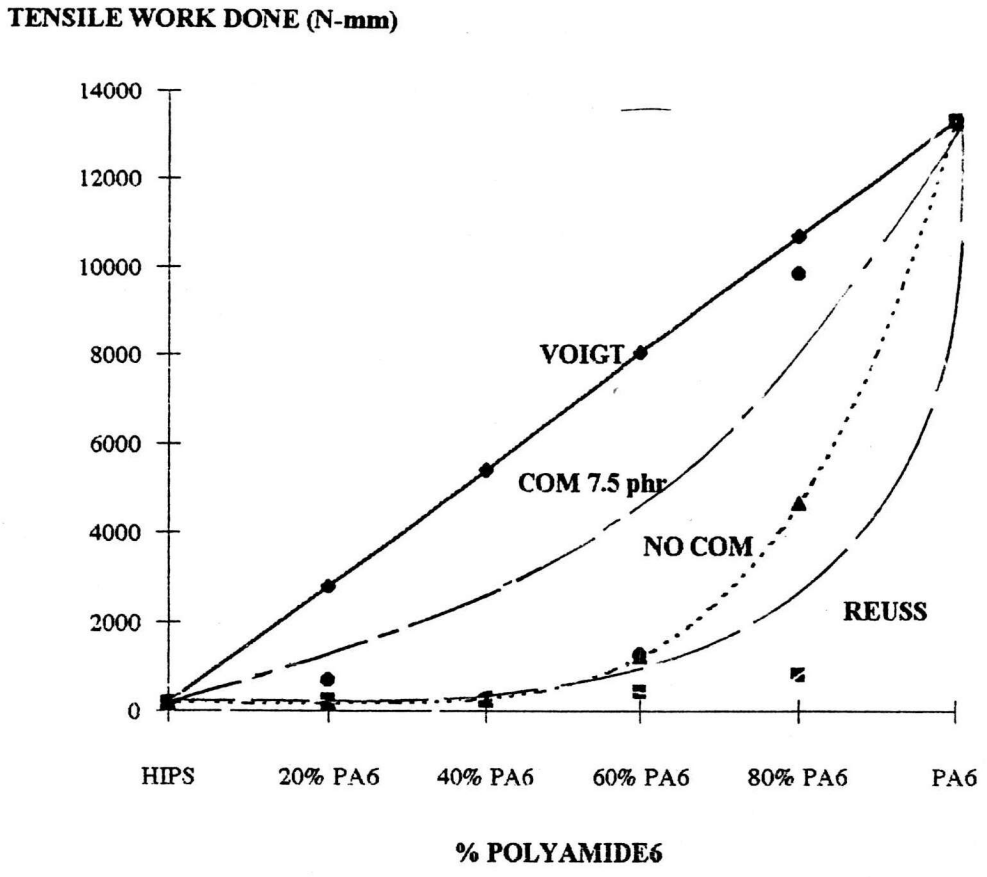

Figure 4.26: The tensile work done of uncompatibilized and compatibilized PA6/HiPS blends plotted against the PA6 concentrations.

From Figure 4.26, the actual tensile work done obtained in the uncompatbilized PA6/HiPS blends shows a little change in range of one-passed HiPS to 60/40 PA6/HiPS blend then it increases dramatically as the PA6 content becomes greater. And it settle between those estimated by Voigt's and Reuss'model.

With the presence of 7.5 phr compatibilizer, the increasing or reduction of the tensile work done depend on the change of tensile

stress at break and tensile strain at break, which is discussed in previous section.

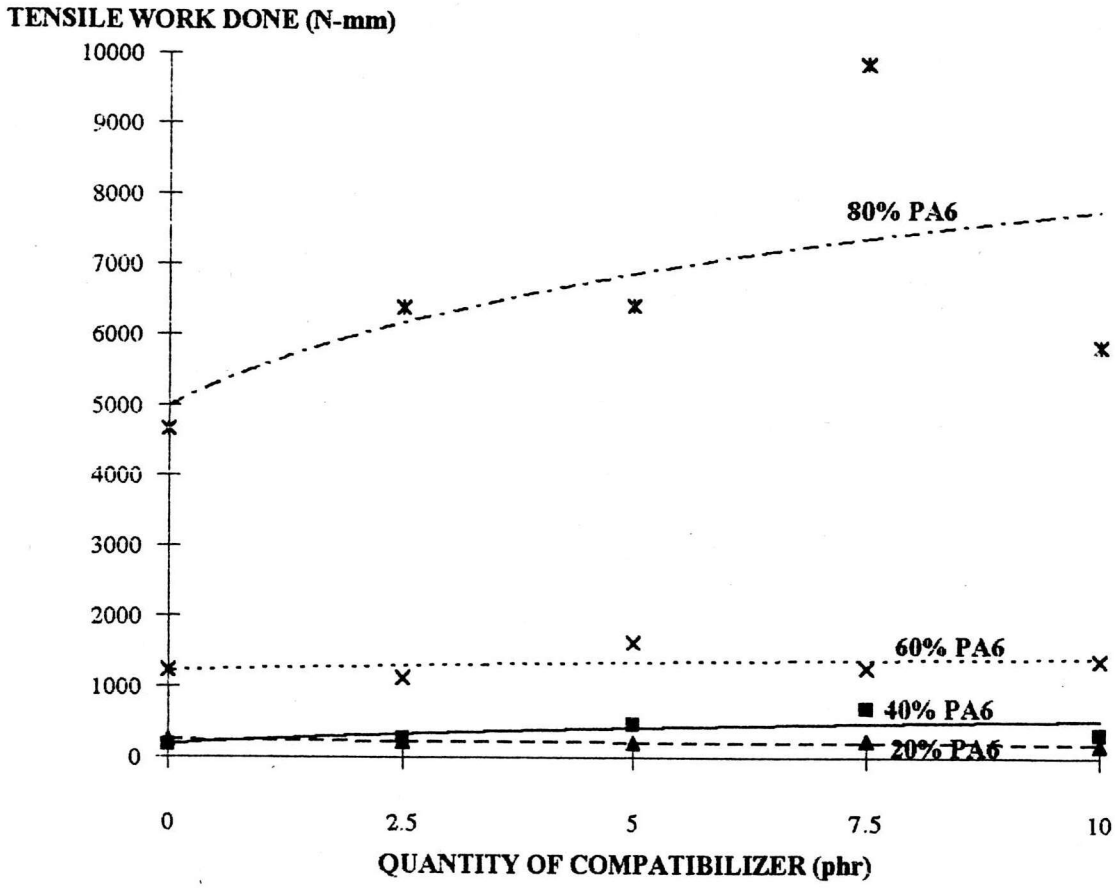

Figure 4.27: The tensile work done of compatibilized PA6/HiPS blends plotted against the SEBS-g-MA concentrations.

As shown in Figure 4.27, the actual tensile work done of 80/20 PA6/HiPS blend with SEBS-g-MA are higher than that of the uncompatibilized 80/20 PA6/HiPS blend. It increases gently over the applied range 0 to 7.5 phr of SEBS-g-MA. After that it decreases a little for 10 phr of SEBS-g-MA. For 60/40 PA6/HiPS blend, the tensile work done have uncertain change when the amount of SEBS-g-MA increases.

For 40/60 PA6/HiPS blend, the addition of SEBS-g-MA decreases the tensile work done. For 20/80 PA6/HiPS blend, over the applied range 0-7.5 phr the more amount of SEBS-g-MA increases, the more the tensile work done increases but with 10 phr of SEBS-g-MA, the tensile work done drops a little from 20/80 PA6/HiPS with 7.5 phr of SEBS-g-MA.

For 80/20 PA6/HiPS blend, when 2.5-10 phr of SEBS-g-MA was added the tensile work done increase by 37, 37.9, 111 and 25.4%. For 40/60 PA6/HiPS blend, when 2.5-10 phr of SEBS-g-MA was added the tensile work done decrease by 8.8, 15, 6.7 and 30%. For 20/80 PA6/HiPS blend, when 2.5-10 phr of SEBS-g-MA was added the tensile work done significantly increases by 56.9, 173.2, 310.8 and 95.4%.

4.2.2.2 Izod impact test

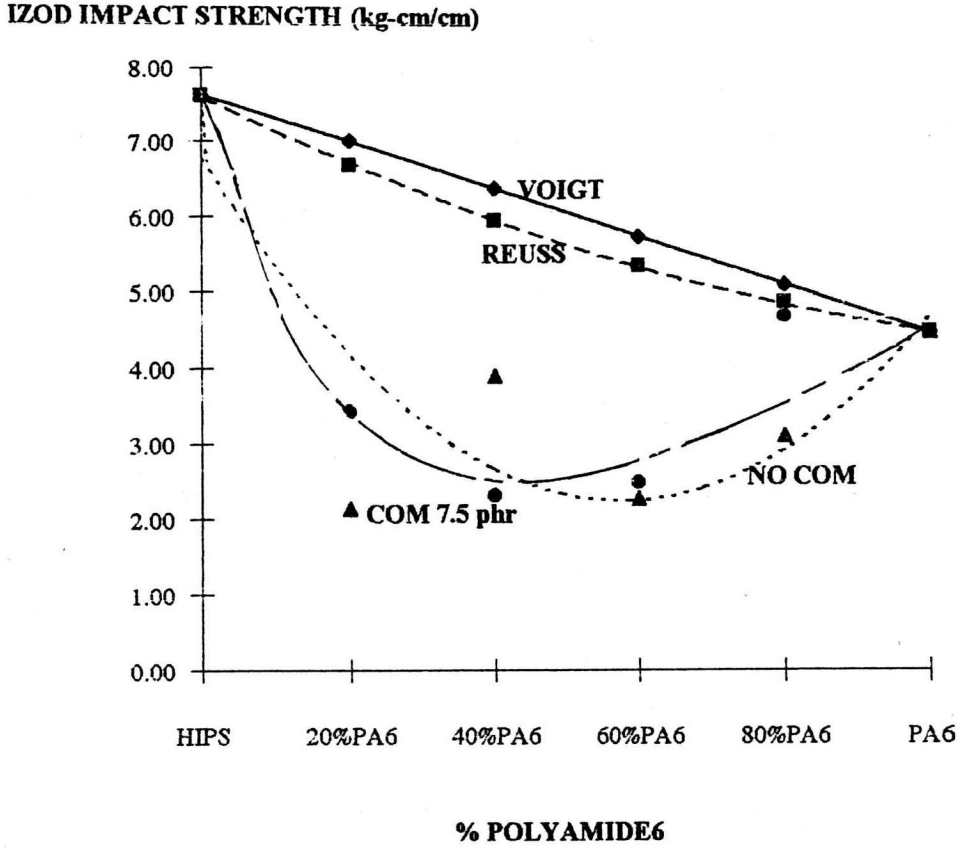

Figure 4.28: The Izod impact strength of uncompatibilized and compatibilized PA6/HiPS blends plotted against the PA6 concentrations.

Figure 4.28 shows that the Izod impact strength of the uncompatibilized blends are lower than those estimated by both Voigt and Reuss' model. The Izod impact strength reduces dramatically from 7.18 kg-cm/cm for one-passed HiPS to 2.13 kg-cm/cm for 20/80 PA6/HiPS blend then it increases gradually to 5.75 kg-cm/cm for one-pass PA6.

Although the domain phase is able to act as a crack-stopper or blunting of the crack tip for PA6 and HiPS respectively, the low interface adhesion causes crack propagation by allowing the crack to pass the weak interface adhesion. The result of the Izod impact strength of 40% PA6 is different from other uncompatibilized blends because the morphology of the domain which is the PA6 phase has fibril structure with a high aspect ratio.

With the presence of the 7.5 compatibilizer, the Izod impact strength trend line changes the minimum point from about 40% PA6 concentration to about 60% PA6 concentration and the Izod impact strength is highered. The increasing of the Izod impact strength is believed to be interface adhesion effect induced by the compatibilizer, which reacts with both the PA6 and the HiPS. The domain phase is able to act as a crack-stopper or blunting of the crack tip for PA6 and HiPS respectively, which is better than uncompatibilized blends. In addition, the better dispersion of domain increases the opportunity for crack tip to meet domain phase, except in 40/60 PA6/HiPS blend, the presence of compatibilizer reduces the domain aspect ratio, so it gives the inverse result.

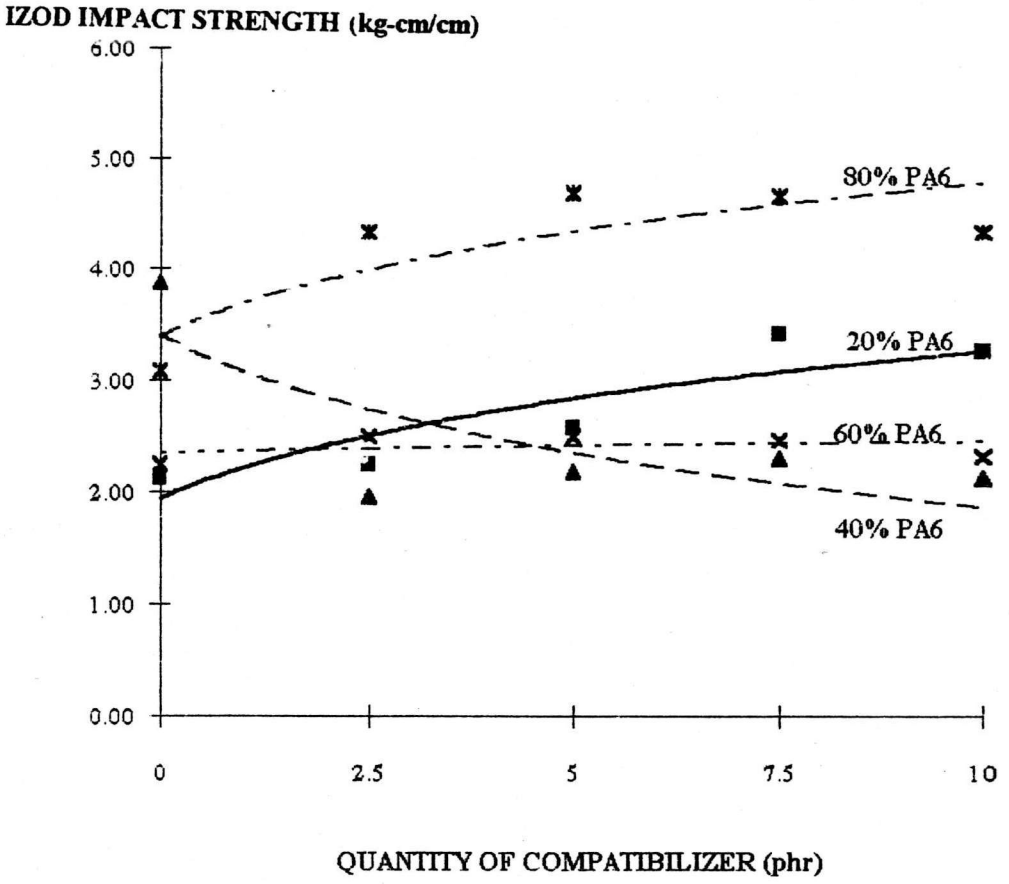

Figure 4.29: The Izod impact strength of compatibilized PA6/HiPS blends plotted against SEBS-g-MA concentrations.

As shown in Figure 4.29, the Izod impact strength of 80/20, 60/40 and 20/80 PA6/HiPS blend are increased by adding SEBS-g-MA. Whereas the Izod impact strength of 40/60 PA6/HiPS blend is decreased by adding SEBS-g-MA.

For 80/20 PA6/HiPS blend, with 2.5, 5, 7.5 and 10 phr SEBS-g-MA, the Izod impact strength increases by 40, 51.5, 50.6 and 40%. For 60/40 PA6/HiPS blend, the more amount of SEBS-g-MA increases, the more the Izod impact strength decreases but all of them are still higher than uncompatibilized 60/40 PA6/HiPS blend. For 60/40

PA6/HiPS blend, with 2.5, 5, 7.5 and 10 phr SEBS-g-MA, the Izod impact strength increases by 11, 11.3, 9.5 and 3%. For 40/60 PA6/HiPS blend, with 2.5, 5, 7.5 and 10 phr SEBS-g-MA, the Izod impact strength decreases by 49.5, 43.5, 40.6 and 45%. For 20/80 PA6/HiPS, the more amount of SEBS-g-MA increases, the more the Izod impact strength increases. With 2.5, 5, 7.5 and 10 phr SEBS-g-MA, the Izod impact strength increases by 5.9, 21.2, 60.4 and 53.2%.

4.2.1.3 Falling-weight test

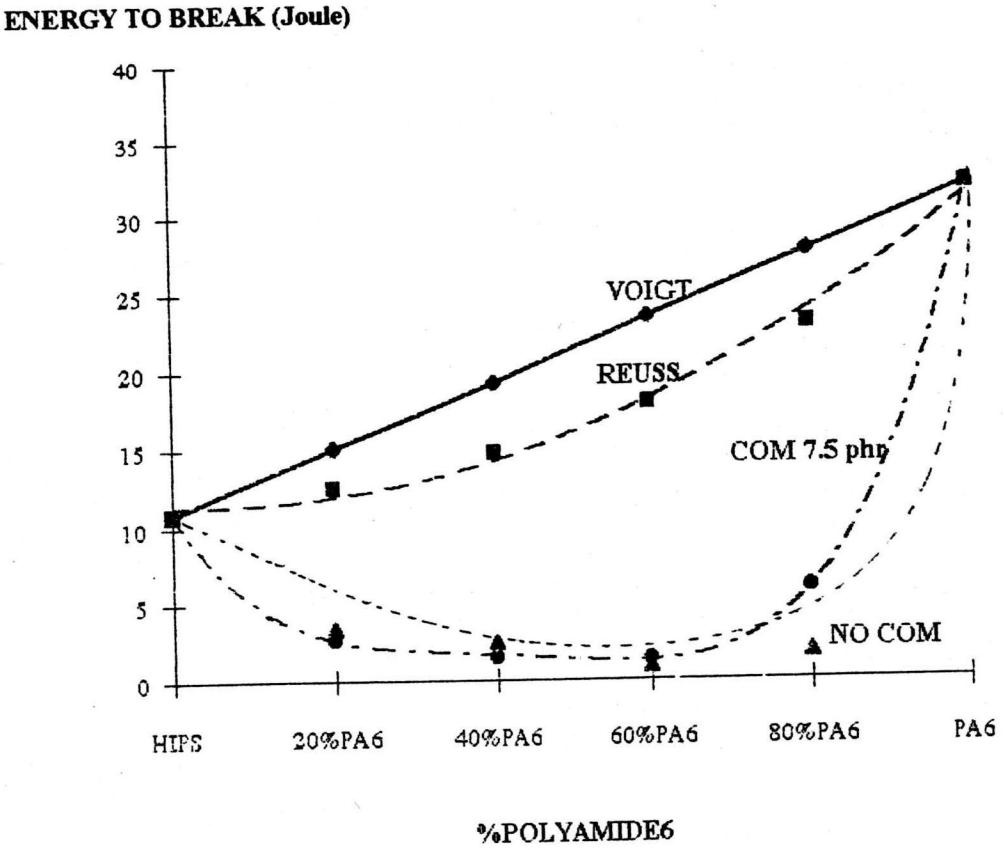

Figure 4.30: The falling-weight energy of uncompatibilized and compatibilized PA6/HiPS blends plotted against the PA6 concentrations.

As it is shown in Figure 4.30, energy to break of falling weight test for every PA6/HiPS ratio are lower than Voigt and Reuss' model. Energy to break decreases sharply from 9.51 J of one-passed HiPS to 3.45 J for 20/80 PA6/HiPS blend. After that energy to break does not change too much between 20/80 PA6/HiPS to 80/20 PA6/HiPS, then, energy to break increases suddenly to 36.51 J for passed PA6.

In addition to the energy to break a plate material, there is test that takes into account the frictional 'push-through' energy term, therefore, besides the interface adhesion, the continuity of blends is important.

The falling weight energy to break of most uncompatibilized blends increases with the presence of the 7.5 phr compatibilizer. The increasing in the falling weight energy is believed to be the interface adhesion and fine dispersion effect. The more interface adhesion and phase dispersion increase, the more the continuity of blends. For the result of 40/60 PA6/HiPS blend, it can be explained in the same way of the Izod impact strength

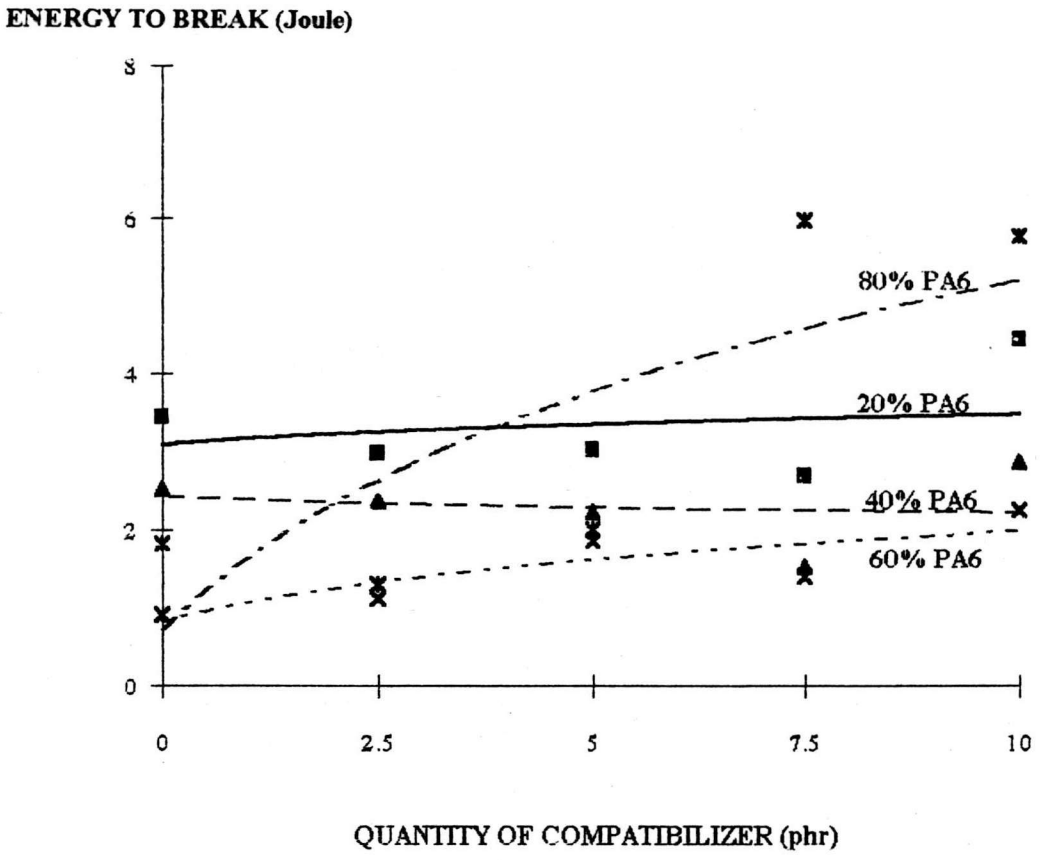

Figure 4.31: The falling-weight impact energy of compatibilized PA6/HiPS blends plotted against the SEBS-g-MA concentrations.

As shown in Figure 4.31, the falling-weight impact energy of 80/20 PA6/HiPS blend does not change significantly in range 2.5-5 phr but when above 5 phr the Falling-weight energy increases sharply. For the 60/40 PA6/HiPS blend the Falling-weight energy increases when compatibilizer was added. For 40/60 and 20/80 PA6/HiPS blend the falling-weight energy don't change significantly.

For 80/20 PA6/HiPS blend, with 2.5 phr of SEBS-g-MA, the Falling-weight energy is decreased by 29.4 but with 5, 7.5 and 10 phr of SEBS-g-MA, the Falling-weight energy are increased by 9.2, 224.5 and 213.6%. For 60/40 PA6/HiPS blend, with 2.5, 5, 7.5 and 10 phr of SEBS-g-MA, the Falling-weight energy are increased by 21.7, 104.4, 52.2 and 146.7%.

4.2.2.4 Heat-distortion temperature; HDT

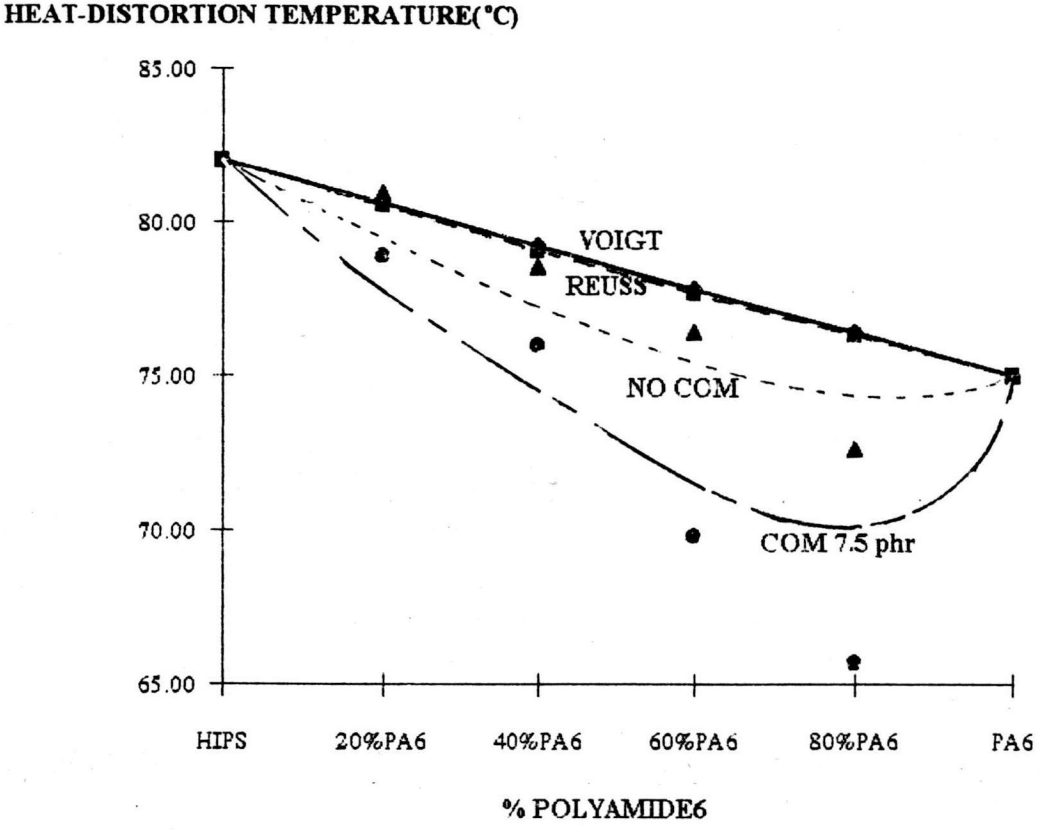

Figure 4.32: The heat distortion temperature of uncompatibilized and compatibilized PA6/HiPS blends plotted against the PA6 concentrations.

The actual HDT in the uncompatibilized PA6/HiPS blends shows a decrease as the PA6 content becomes greater. Figure 4.32 shows that the HDT of uncompatibilized PA6/HiPS blends are lower than those estimated by Voigt and Reuss' model.

The HDT is directly related to the glass-transition temperature of the polymer and the content of additive. So the increase of PA6 content which has lower glass-transition temperature than PS; the matrix of HiPS, then the HDT of uncompatibilized blends will be decreased.

In the same way, the addition of compatibilizer in PA6/HiPS blends reduces the HDT of these blends because the compatbilizer has the lowest glass-transition temperature.

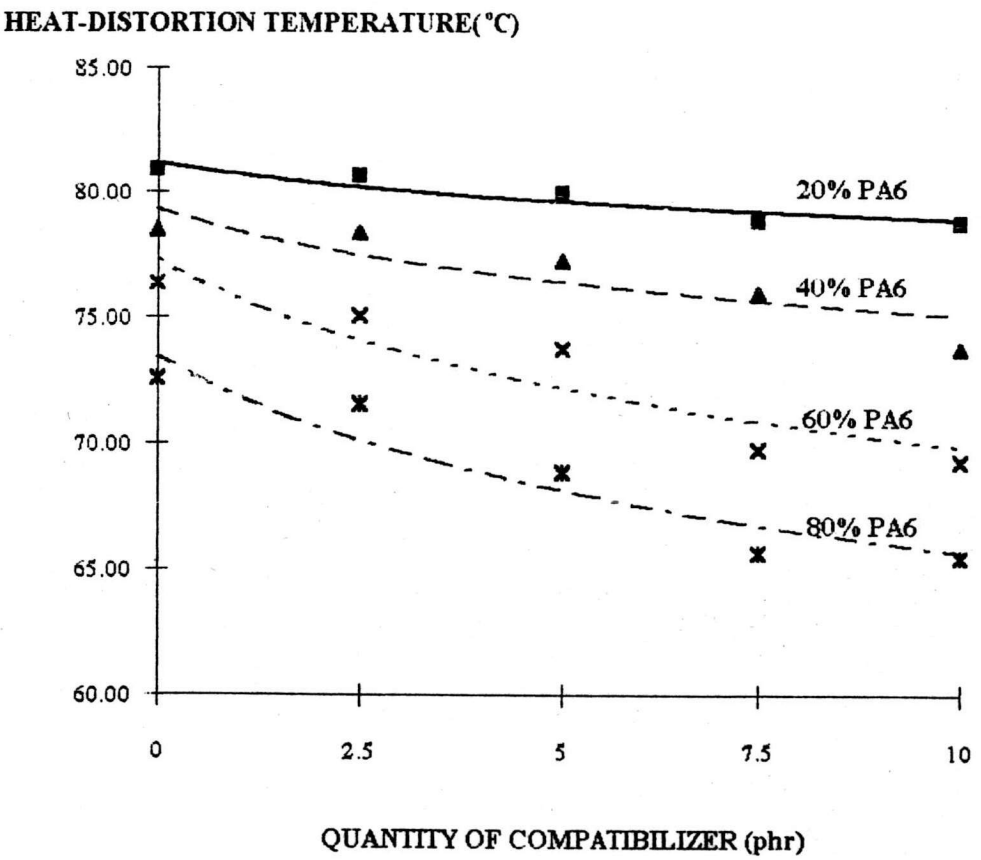

Figure 4.33: The heat-distortion temperature of compatibilized PA6/HiPS blends plotted against the SEBS-g-MA concentrations.

As shown in Figure 4.33 the HDT of all blend decreased when adding the SEBS-g-MA. The more quantity of SEBS-g-MA increases, the more HDT decreases.

For 80/20 PA6/HiPS blend, with 2.5, 5, 7.5 and 10 phr of SEBS-g-MA, the HDT decreases by 1.4, 5.1, 9.5 and 9.8%. For 60/40 PA6/HiPS blend, with 2.5, 5, 7.5 and 10 phr of SEBS-g-MA, the HDT decreases by 1.7, 3.4, 8.1 and 9.3%. For 40/60 PA6/HiPS blend, with 2.5, 5, 7.5 and 10 phr of SEBS-g-MA, the HDT decreases by 0.1, 1.5, 3.2 and 6%. For 20/80 PA6/HiPS blend, with 2.5, 5, 7.5 and 10 phr of SEBS-g-MA, the HDT decreases by 0.2, 1.1, 2.5 and 2.6%.

4.3 Characterization

This section shows the trend of compatibility, percentage of crystallinity of PA 6 and morphology of the blends. The compatibility is determined by using Dynamic Mechanical Thermal Analysis (DMTA) and Scanning Electron Microscope (SEM). The crystallinity and melting point temperature of PA 6 in blends are determined by using Differential Scanning Colorimeter (DSC).

4.3.1 Density

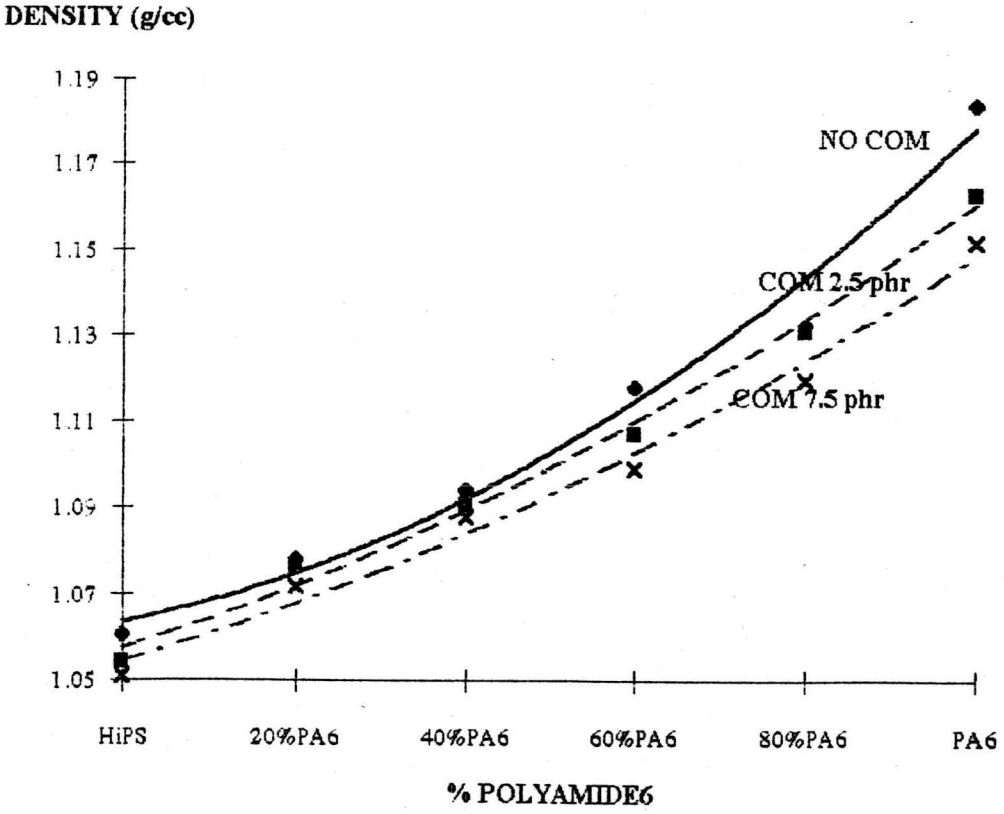

Figure 4.34: The density of blend against the percentage of polyamide 6.

Figure 4.34 shows that the density of the blends decreases when the amount of the SEBS-g-MA compatibilizer increase. As more amount of SEBS-g-MA was added, the sharper is the decrease in the density of the blend.

4.3.2 Dynamic Mechanical Thermal Analysis (DMTA)

Pure HiPS exhibits two transitions characterized by the temperature of the tan δ on the plot of tan δ versus temperature. The low temperature transition at about -72.6 °C corresponds to the glass transition of the rubber phase. The high temperature transition at 120.9 °C is the glass transition temperature of the matrix polystyrene (PS) phase of the HiPS. The transition corresponds to the amorphous part of the polyamide 6 (PA6) is localized near 70.8 °C. The low temperature transition of PA6 at -57.87 °C is believed to be due to the presence of a small amount of water.

Figure 4.35 shows the compositional dependence of the glass transition temperature (T_g) of each constituent for the unompatibilized PA6/HiPS blends with and without the compatibilizer. For the PA6/HiPS blends without compatibilizer, the glass transition temperatures of the PA6, PS and PB in the HiPS are dependent on the blends composition. The glass transition temperature of the PS in the HiPS decreases slightly whereas that of the rubber (PB) in the HiPS increases slightly when the percentage of the PA 6 composition increased up to 100%. The T_g of the amorphous part of the PA6 gradually increases when the PA 6 amout decreases. For a low amount of PA6, the tan δ peak of the amorphous part is overlaid by the tan δ peak of the PS.

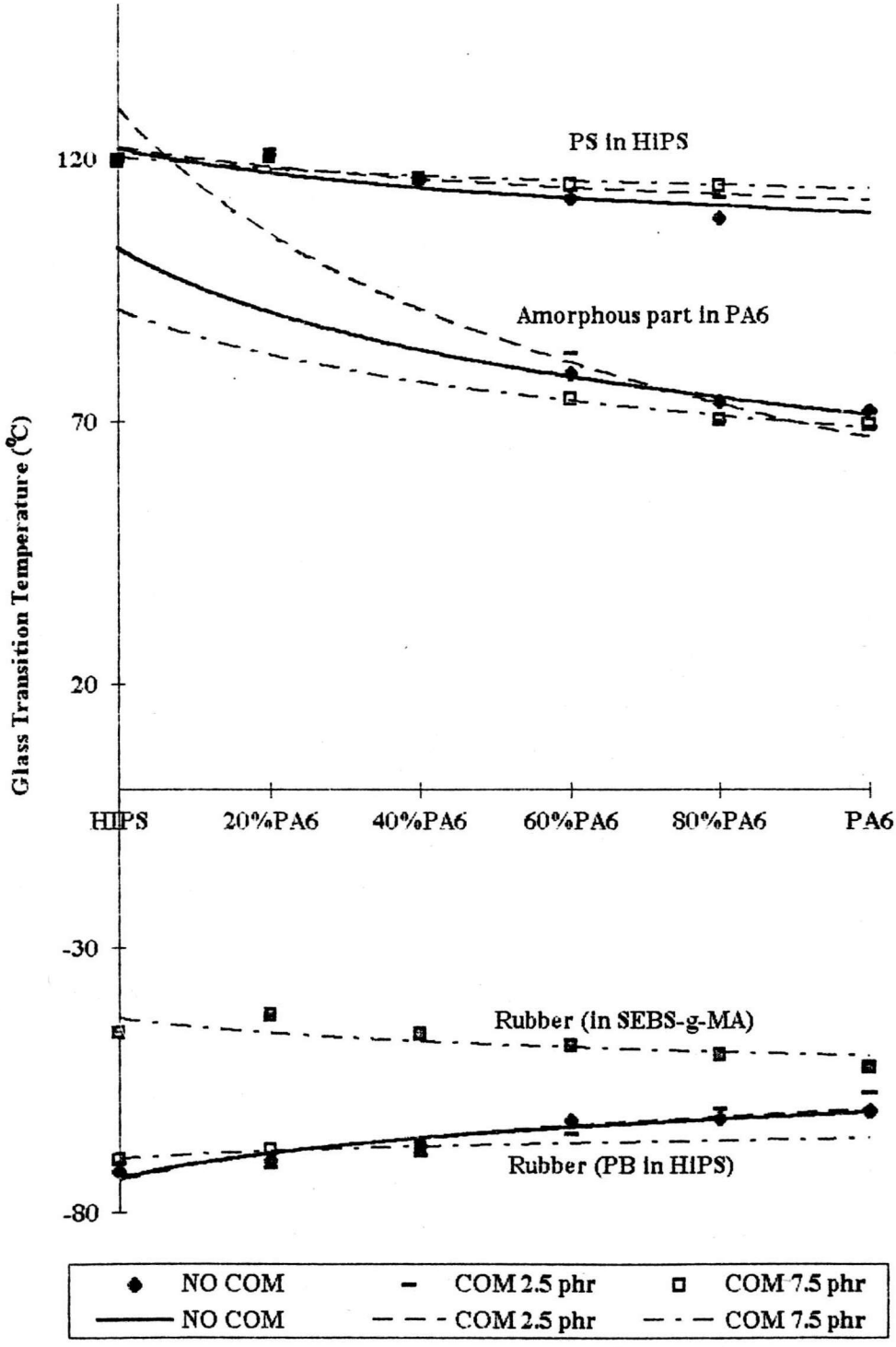

Figure 4.35: The glass transition temperature (T_g) of each component for the PA6/HiPS blends with and without a compatibilizer plotted against the percentage of Polyamide 6.

For the compatibilized PA6/HiPS blends with SEBS-g-MA 2.5 phr, the glass transition temperatures of the PA6, PS and PB in the HiPS are dependent on the blends composition. This is a clear indication that the PA6/HiPS blends are partially miscible blends, as will be verified by the presence of the two phases in the fractography study in Section 4.3.4. The glass transition temperature of the PS in the HiPS is slightly higher than those in the uncompatibilized blends whereas the T_g of the rubber in HiPS is nearly the same as the uncompatibilized one. However, the trend line of PS and rubber are in the same direction with the uncompatibilized blends. The T_g of the amorphous part of PA6 sharply increases when the PA 6 composition decreases. It is also close to that of the PS and higher than the T_g of PS in the incompatible blends. However, at the range higher than 60 % composition of PA6, the T_g of the amorphous part of PA6 is lower than the uncompatibilized PA6/HiPS blends.

For the compatibilized PA6/HiPS blend with SEBS-g-MA 7.5 phr, the glass transition temperature of the PA6, the PS and the PB in HiPS are varied by the blend compositions. The new tan δ peak when SEBS-g-MA is present are at about -45.98 to -52.58 °C. These peaks are expected to be the peak of the rubber and styrene respetively in the SEBS-g-MA. In additional, these peaks show the presence of the fourth phase in PA6/HiPS blends.

The glass transition temperature of PS in the compatibilized PA6/HiPS blends with compatibilizer 7.5 phr decreases slightly when the % PA 6 composition increases up to 100%. However the T_g with the 7.5

phr decreases at a lower rate than that of the systems with 2.5 phr. The T_g of the rubber in HiPS with 7.5 phr is higher than that with 2.5 phr. At the range where the composition of HiPS is small, the tan δ peak of the rubber in HiPS becomes shoulder of the new peak.

At the composition range of 60/40 to 100/0 PA 6/HiPS blends, the T_g of the amorphous part of the PA 6 decreases at a rate slower than those of both the uncompatibilized and the compatibilized blends with SEBS-g-MA 2.5 phr, also the T_g is lower than those of both systems.

It is clearly shown in Figure 4.35 that there is no single T_g for all types of composition. This is a clear evidence the PA6/HiPS blends are not missible. The PA6 and HiPS did not mix at their molecular level despite an addition of the SEBS-g-MA compatibilizer. However, by adding the compatibilizer at 2.5 phr, there is a sharp increase in the T_g of the amorphous part of PA6 when the PA 6 composition is low. Hence the effect of the SEBS-g-MA is more prominent in the amorphous part of PA6.

4.3.3 Differential Scanning Colorimeter (DSC)

For the glass transition temperature of PS in HiPS, the melting point of fusion and heat of fusion (ΔH_m) was determined by using a Differential Scanning Colorimeter (DSC). The DSC thermogram for the PA6/HiPS blends are shown in Figures 4.36 to 4.38.

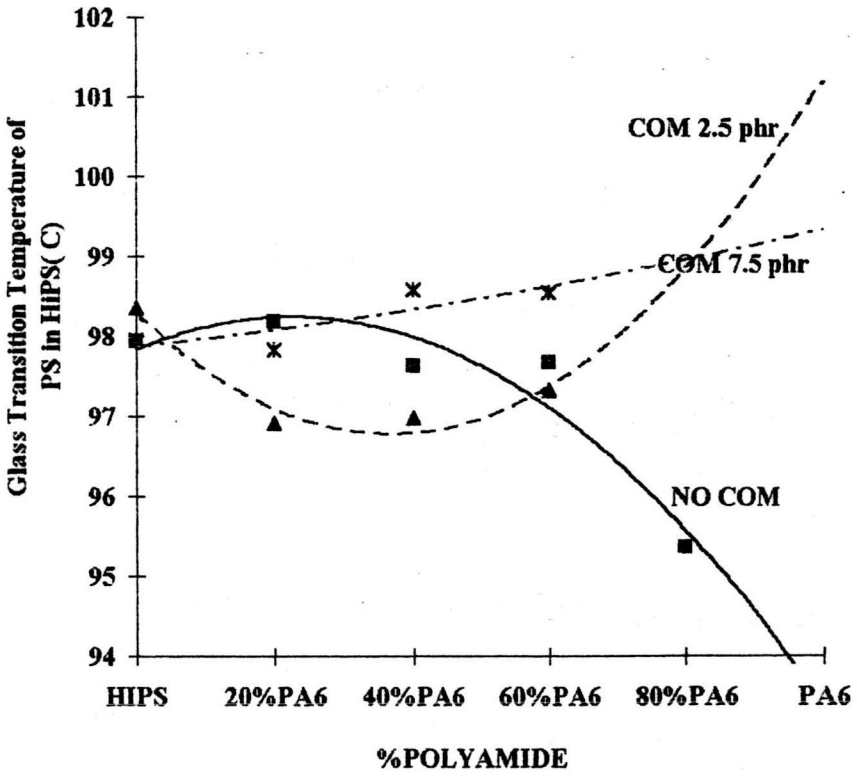

Figure 4.36: The glass transition temperature of PS in HiPS is plotted against the percentage of Polyamide 6 in the PA6/HiPS blends.

From Figure 4.36, the glass transition temperature of PS in the HiPS with different amount of compatibilizer shows a trend similar to that from the DMTA test. The T_g of the PS in the uncompatibilized

blends decreases faster than that in the compatibilized blends with SEBS-g-MA 2.5 phr. For the compatibilized PA6/HiPS blends with SEBS-g-MA 7.5 phr, the T_g tends to increase. The more the amount of the compatibilizer, the higher is the glass transition temperature. This is believed to be the effect of the compatibilizer acting as a constrain and delay the mobility of the PS chain in HiPS. As a result, the PA6/HiPS with higher concentration of SEBS-g-MA requires greater amount of thermal energy for the chain mobility to be initiated.

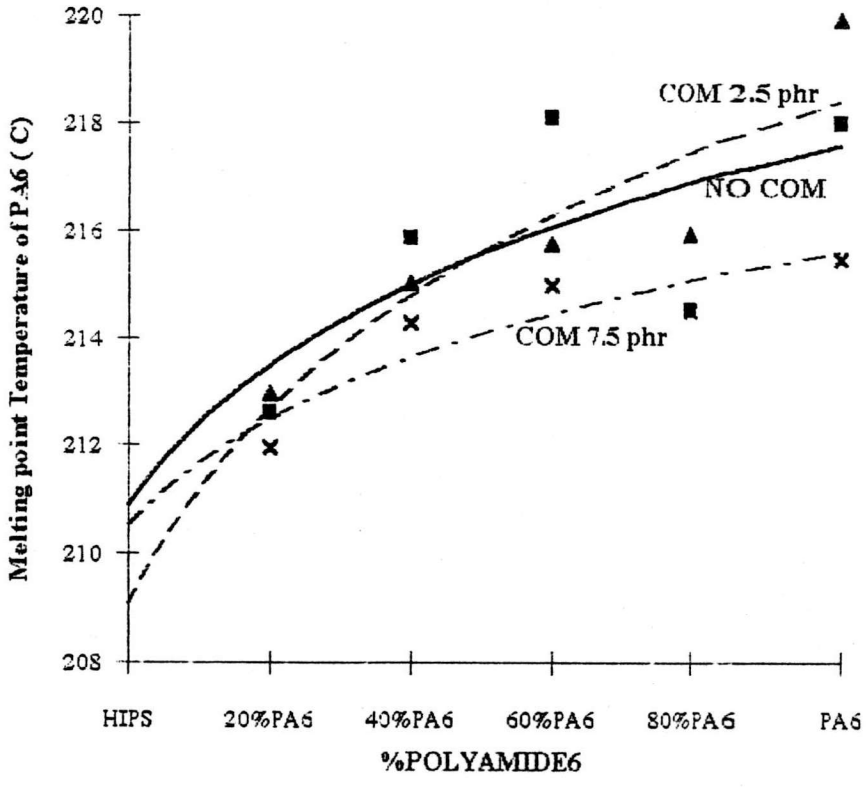

Figure 4.37: The melting point of Polyamide 6 in PA6/HiPS blends is plotted against the percentage of Polyamide 6.

From Figure 4.37, the melting point of PA6 increases when the percentage of PA6 in the blends increases. At 7.5 phr of SEBS-g-MA, the melting point of the blends are decreased. This may be due to the reaction of compatibilizer with the CONH in the PA6 and hence reduce Hydrogen-bond in PA6. With more compatibilizer in the system, there is more nucleating site for the PA6 crystallize. This resultant crystallites may be smaller in size and the degree of crystallinity may also be reduced.

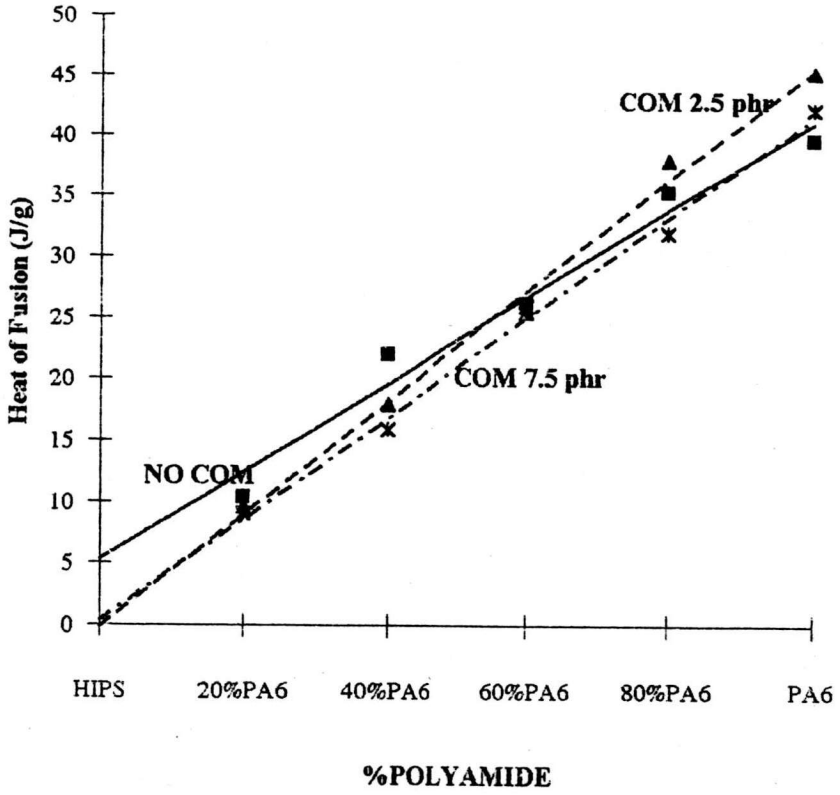

Figure 4.38: The heat of fusion is plotted against the percentage of Polyamide 6 in the PA6/HiPS blends.

Figure 4.38 shows that the heat of fusion is almost a linear function of the blend composition. The crytallinity (X_c) of the PA6 phase is calculated by means of the following relation:

$$X_c = 100\ \Delta H_{blend}/(\Delta H^{\circ}_{PA6} X \text{ weight fraction of PA6})$$

where ΔH_{blend} is the heat of fusion per gram of the blend

ΔH°_{PA6} is the heat of fusion per gram of 100% crystalline PA6 [11]

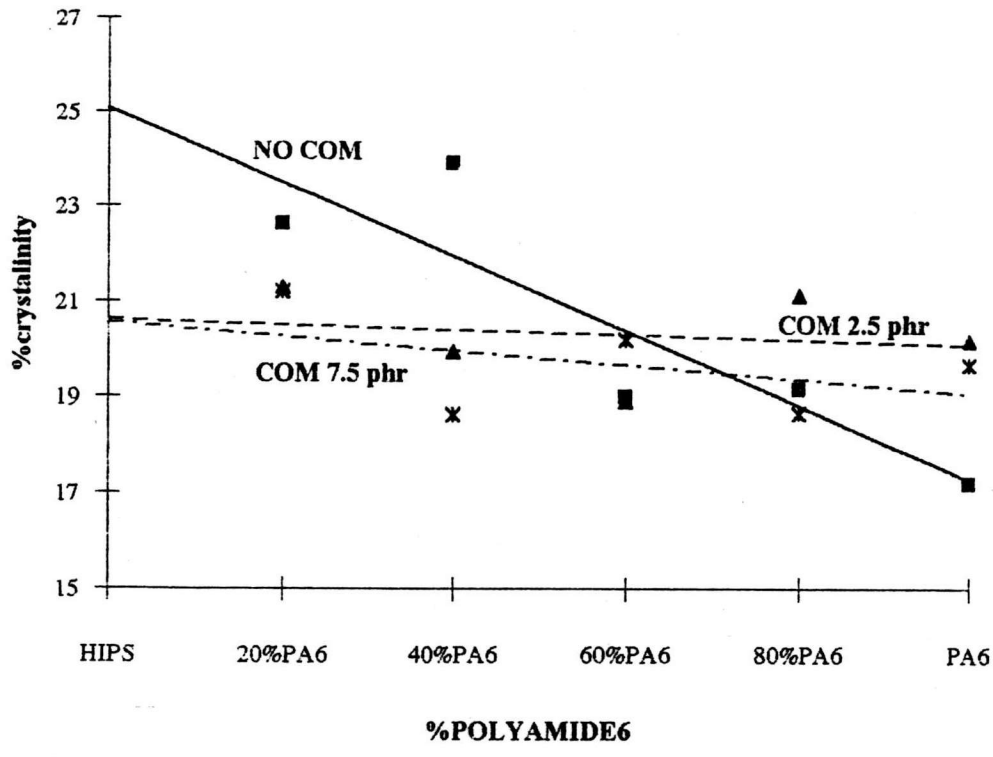

Figure 4.39: Crystallinity of the polyamide 6 against the percentage of Polyamide 6

From Figure 4.39, in uncompatibilized blend, the more percentage of PA6 increases, the more crystallinity of PA6 decreases. However, by adding the compatibilizer to the blends, the percentage of crystallinity at various composition of PA6 seems to vary in the narrow range between 19 to 21. The different of slope between the uncompatibilized and the compatibilized blends can be explained by the formation of graft copolymer, there is a reaction of amide ended groups of PA 6 with maleic anhydride in the SEBS-g-MA. For the compatibilized blends, the crystallinity of PA 6 seems to be independent of blend composition. This stability of crystallinity may be due to the existence of HiPS phase.

4.3.4 Fractography

This section is to observe the blend morphology at different composition of polyamide PA6 and HiPS. The phase morphology is, no doubt, a very important aspect of the properties of polymer blends; however, the scanning electron microscopy techniques used in this study lead to only a rather limited understanding.

The morphology of the incompatible blend is illustrated in Figure 4.40, with varied composition between PA6/HiPS as follows: (a) 20/80 (b) 40/60 (c) 60/40 and (d) 80/20. It can be seen that these morphology are coarse dispersion and poor distribution. In addition, from Figure 4.40 (b), the polymer blend have fibril domain, so it confirms our expect about some mechanical property of this composition which is inconsistent with the other compositions.

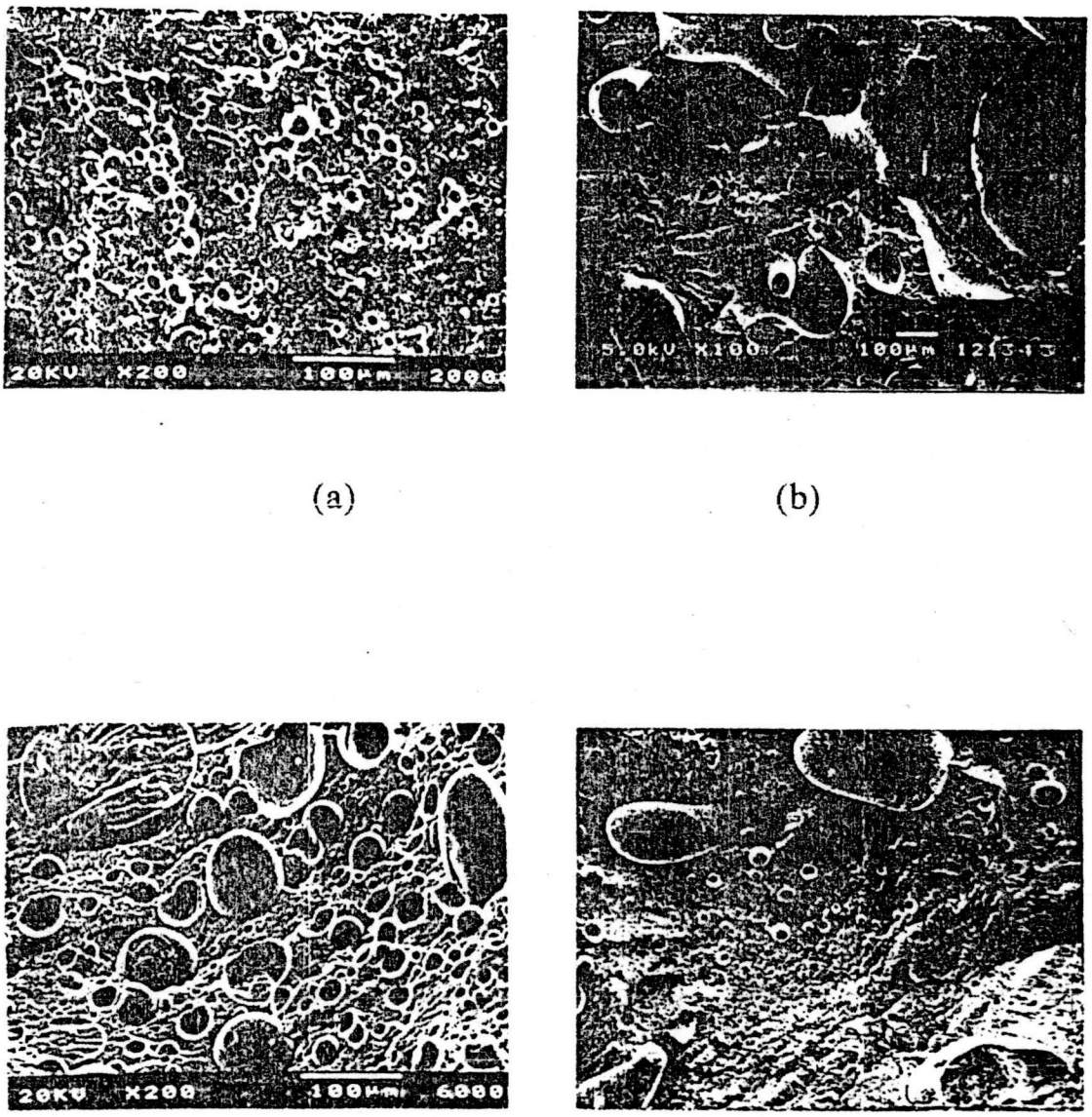

(a) (b)

(c) (d)

Figure 4.40: The morphology of incompatible blend at different composition of PA6 and HiPS

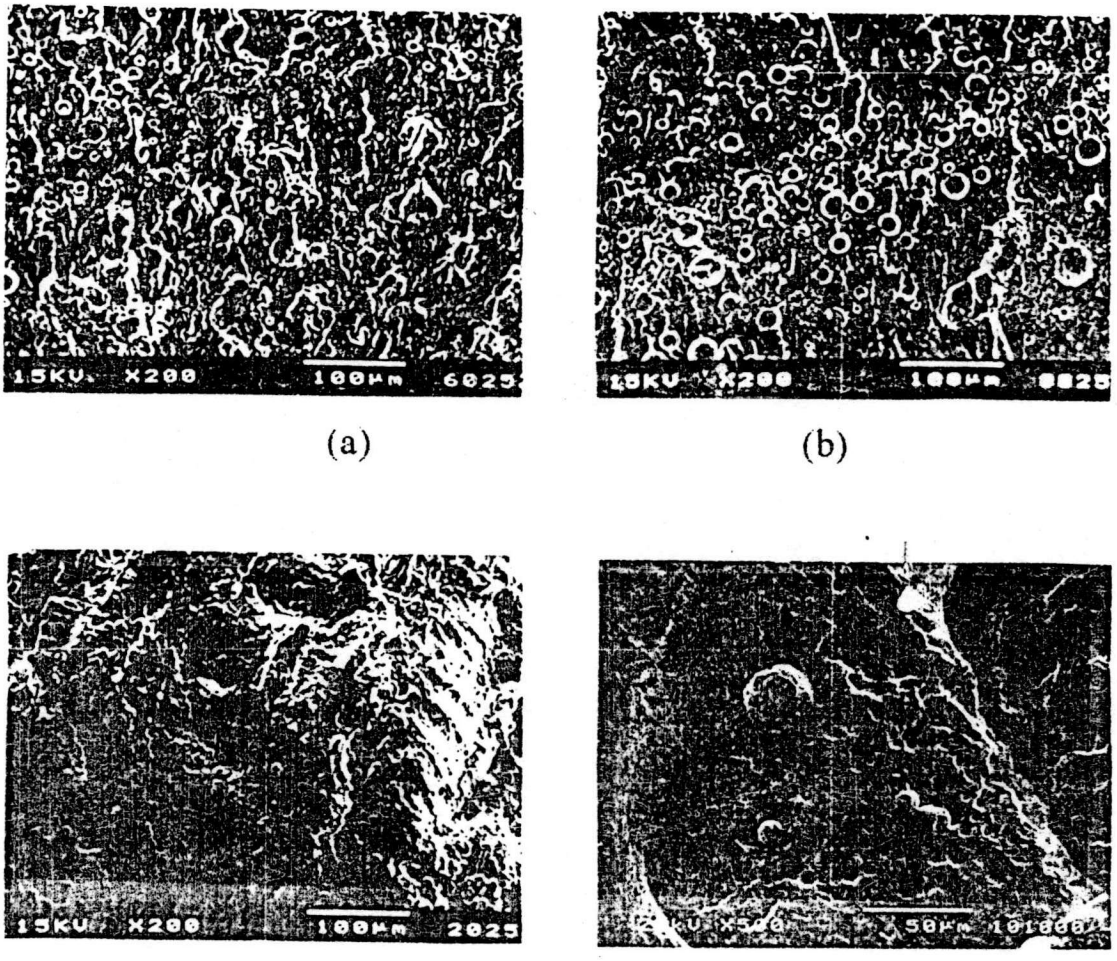

Figure 4.41: The morphology of compatible blend with 2.5 phr of SEBS-g-MA.

When adding 2.5 phr of SEBS-g-MA to the blends, the dispersion and distribution of blends morphology was .clearly improved which can be seen in Figure 4.41. It was expected that formation of graft copolymer at the interface should result in a decrease in domain size through lowering of interfacial tension.

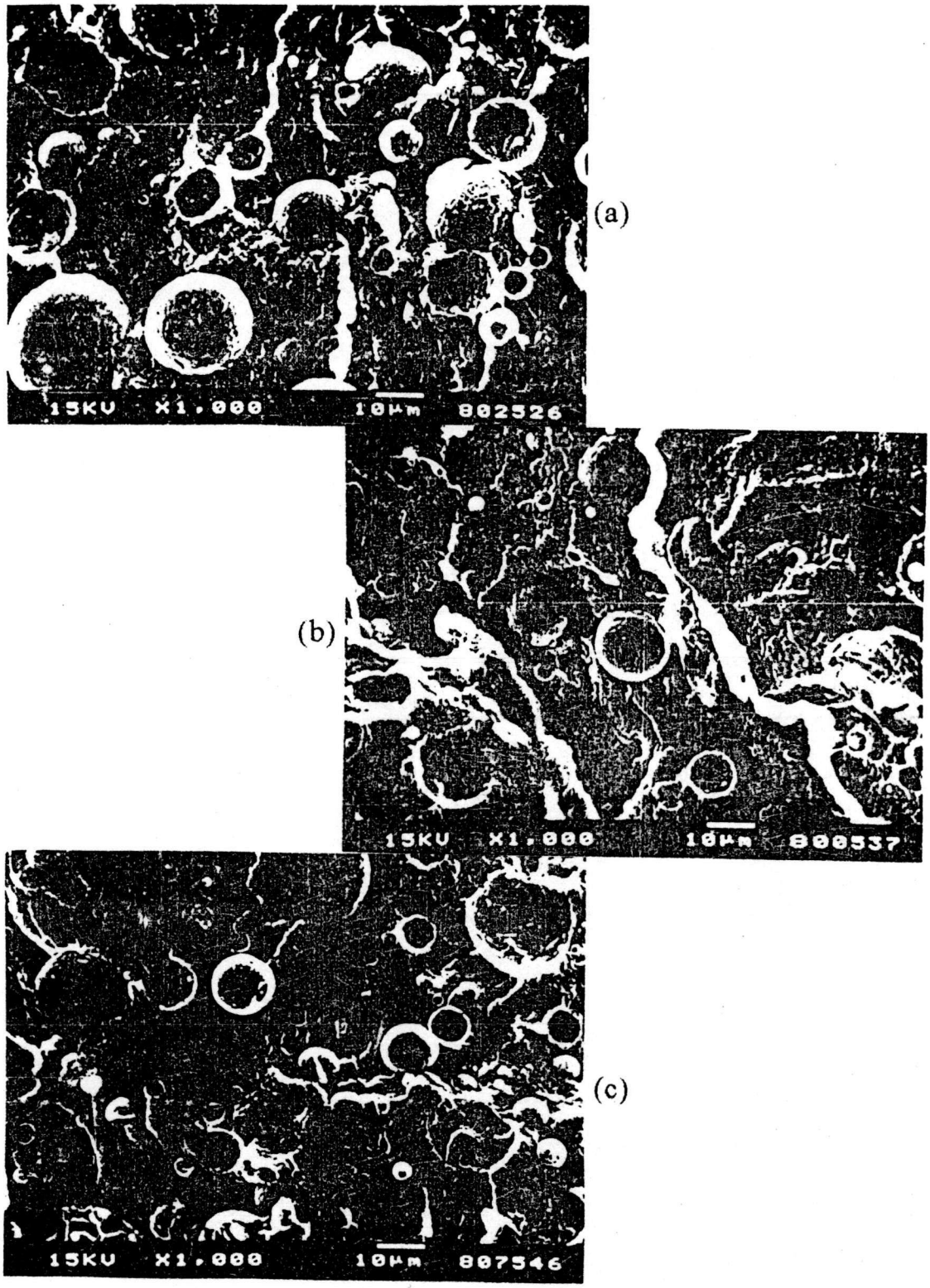

Figure 4.42: The morphology of compatible blend of composition of PA6/HiPS 80/20 with 2.5 to 7.5 phr of SEBS-g-MA

Figure 4.42 shows the effect of SEBS-g-MA from 2.5 to 7.5 phr to the morphology of PA6/HiPS 80/20, the domain size is reduced by the adding of SEBS-g-MA from 2.5 to 5 phr, as shown in figure 4.42 (a) and (b). When adding SEBS-g-MA from 5 to 7.5 phr to this blend, as shown in Figure 4.42 (b) and (c), the domain size is continually reduced. However, in Figure 4.42 (c), it seems to have two dispersion size of domain.

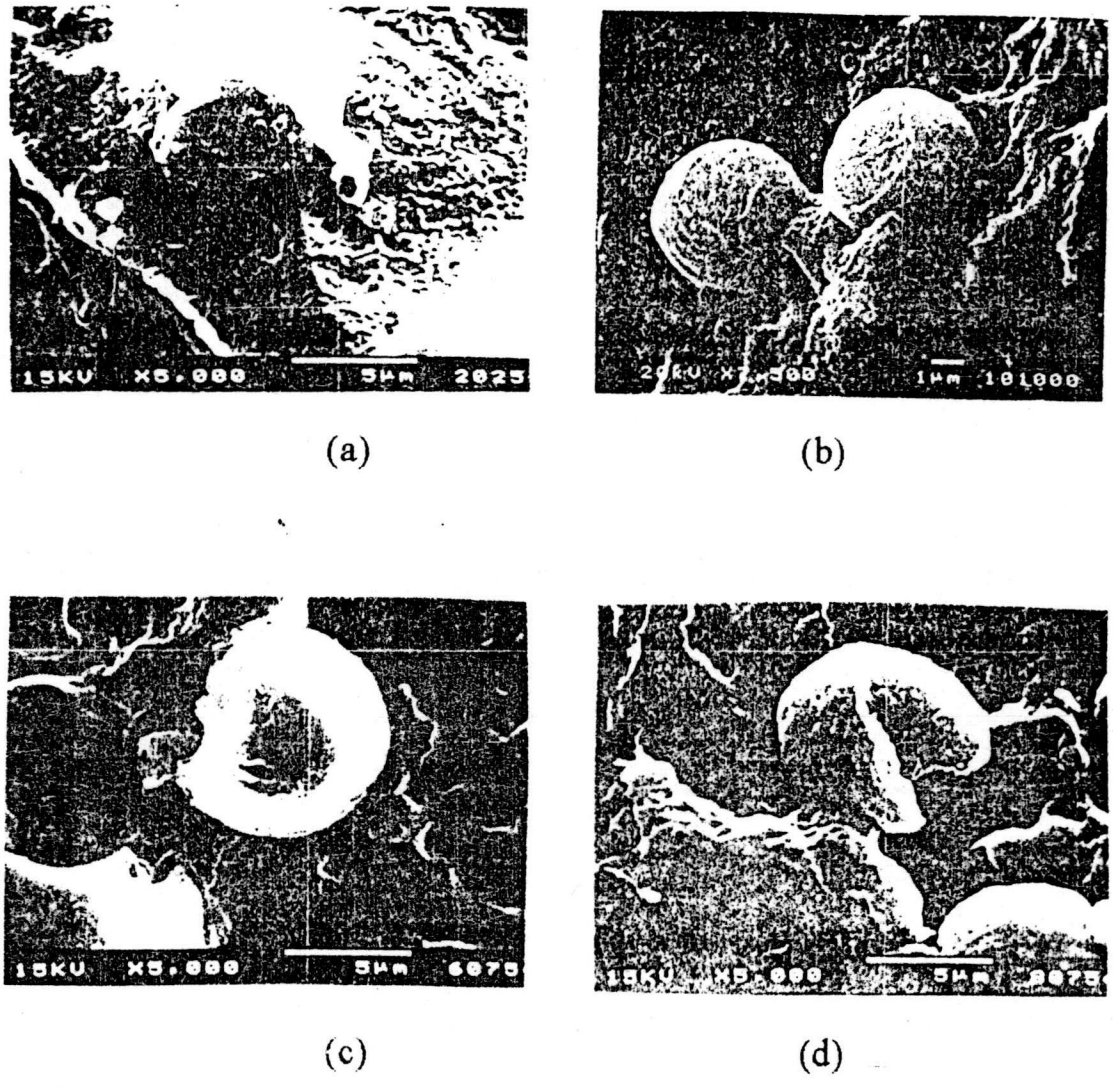

(a) (b)

(c) (d)

Figure 4.43: The morphology of compatibilized blends when using high magnification.

By using high magnification to observe the adhesive of domain and matrix, in Figure 4.43 (a) and (b), it can be seen that the domain seems to be tough while in Figure 4 (c) and (d), the domain have fracture. Therefore, it can be concluded that at (a) and (b) the dispersion phase is PA6 while at (c) and (d) the dispersion phase is HiPS.